AGU ADVANCING EARTH AND SPACE SCIENCE

Water Resources Research

RESEARCH ARTICLE
10.1029/2020WR028133

Representing Human Water Management in a Land Surface Model Using a Supply/Demand Approach

Xudong Zhou[1,2,4], **Jan Polcher**[1], **and Patrice Dumas**[3]

[1]Laboratoire de Météorologie Dynamique, IPSL, CNRS, Ecole Polytechnique, Palaiseau, France, [2]State Key Laboratory of Hydrology-Water Resources and Hydraulic Engineering, Hohai University, Nanjing, China, [3]CIRAD, UMR CIRED, Montpellier, France, [4]Now at University of Tokyo, Meguro-ku, Japan

Key Points:

- Human water management is developed to represent water usage and regulation by dams in a land surface model
- A forest of river graphs is introduced for the routing and adduction network to represent the supply demand path and demand propagations
- Implementation over the Yellow River basin reveals improved model performance in seasonality and spatial heterogeneity of river flows

Supporting Information:

Supporting Information may be found in the online version of this article.

Correspondence to:

J. Polcher,
jan.polcher@lmd.jussieu.fr

Citation:

Zhou, X., Polcher, J., & Dumas, P. (2021). Representing human water management in a land surface model using a supply/demand approach. *Water Resources Research*, *57*, e2020WR028133. https://doi.org/10.1029/2020WR028133

Received 13 JUN 2020
Accepted 6 MAR 2021

Author Contributions:

Conceptualization: Jan Polcher
Data curation: Xudong Zhou
Formal analysis: Xudong Zhou
Methodology: Jan Polcher, Patrice Dumas
Software: Xudong Zhou
Supervision: Jan Polcher
Writing – original draft: Xudong Zhou
Writing – review & editing: Jan Polcher, Patrice Dumas

Abstract The impact of human water management on river discharge is increasingly viewed as a missing process in Earth system modeling. Models which have attempted to include it are generally at coarse resolution and uncoupled to the atmosphere. We propose to describe human water management at high spatial resolution using ORganizing Carbon and Hydrology In Dynamic EcosystEms concept of hydrological-transfer-units in the routing parametrization. Irrigated areas are linked to river abstraction points using a minimization process. The directed graphs of river flows and adduction network for irrigation is transposed to propagate water demands upstream. Reservoirs and dams are placed along the graph to balance supply and demands in the four chosen water value classes. Dam regulation is assumed to maximize demand satisfaction and dampen floods while respecting the properties of the infrastructure. The developed human water management module is applied to the Yellow River where irrigation and dam regulation are known to have a strong impact. Results show that the impact of human water management is strongly heterogeneous over space. It propagates along the river channels and can be mitigated by the confluence of tributaries. Moreover, the human impact has a strong seasonality due to time varying irrigation demands and the response of dam regulation. A number of uncertainties still remain and affect the simulated river discharge. Nevertheless, the representation of human water management improves the model's behavior in terms of magnitude and intra-annual variations of river discharge, and offers the opportunity to implement anthropogenic processes in the water cycle of Earth System Models.

1. Introduction

Human water management is known to be an important factor that has altered natural river discharge in most large rivers (Jaramillo & Destouni, 2015; Wada et al., 2017). Irrigation represents ~90% of all consumptive water use globally, decreasing the total annual continental runoff by about 7% (Rost et al., 2008; Scherer & Pfister, 2016). Meanwhile, reservoirs and dam releases change the timing of river discharge by reducing extreme flows (flooding and lowest flows), to cover environmental requirements (Biemans et al., 2011; Hanasaki et al., 2006) and meet human water demands. An optimized water management allows to increase agricultural production and bring relief from water scarcity. As a consequence, current flows of rivers can be very different from their natural state.

Irrigation and dam regulation combine with climate variability and change at various temporal and spatial scales to produce the observed river discharge (Pokhrel et al., 2016; Vicente-Serrano et al., 2019). Understanding the contribution of these various factors to the observed changes in the continental water cycle is a scientific challenge which requires innovative hydrological or land surface models (LSM) which incorporate human water managements (Wada et al., 2017). A number of large-scale models (e.g., global, continental scale) have integrated the irrigation schemes using different methodologies. Though, some of these irrigation schemes are uncoupled from the other components of the Earth system due to limitations of global hydrological models in representing the interactions with the atmosphere (Döll & Siebert, 2002; Hanasaki et al., 2018; Rost et al., 2008; Yoshikawa et al., 2014). Some are integrated in LSMs or so-called Earth system models (de Rosnay et al., 2003; Guimberteau, Laval, et al., 2012; Leng et al., 2017; Lobell et al., 2009).

In addition to the irrigation module, Hanasaki et al. (2006) introduced for the first time an algorithm for setting operating rules for individual reservoirs in a global river routing model, which was then incorporated into a global hydrological model named H08 in Hanasaki et al. (2008, 2010). Haddeland et al. (2006)

incorporated a reservoir model with irrigation scheme within the framework of the Variable Infiltration Capacity model with release functions which are optimized with known future inflows. The two approaches have been improved and applied to other models in the last decade (Adam et al., 2007; Biemans et al., 2011; Döll et al., 2009; Voisin et al., 2013). In general, these models with irrigation and dam regulation have shown to provide more accurate simulations of discharge. Furthermore, taking into account dam regulation allows to more adequately satisfy water demands from the different sectors. To our knowledge, dams regulation hasn't yet been introduced into a LSMs because in particular this introduces a new spatial scale which is smaller than the typical atmospheric resolution used in climate models.

Incorporating human water management into LSMs needs a high and consistent spatial resolution in order to preserve hydrological continuity. The spatial resolution of LSMs is always coarse and limited by the atmospheric variables, typically at 0.5° for large-scale implementations (Flato et al., 2014). However, the human influence is at a much higher spatial resolution with an extent of irrigation or urban areas typically limited to a few kilometers. Although the irrigation demand is estimated on a fraction of the cropland within an atmospheric grid using the vegetation tiling approach, the total irrigation demand is treated as an aggregation (Hanasaki et al., 2010; Müller Schmied et al., 2021). Depending on the routing method in existing schemes, individual dams within the same grid are aggregated (Haddeland et al., 2006), and the combined effect of dams along the river segment is only considered in an aggregated way (Lehner et al., 2011). Similarly, the location of irrigated areas relative to surface water availability is lost in LSMs because the tiling approach used in LSMs to represent sub-grid variability is statistical.

In the above mentioned hydrological models with dam regulation (Döll et al., 2009; Haddeland et al., 2006; Hanasaki et al., 2008; Müller Schmied et al., 2021; van Beek et al., 2011), dams serve water for the downstream demands within a certain distance. The maximum distance is user-defined, by the number of model grids or a distance water can travel assuming a given flow velocity, for example 7 days at 1.0 m s^{-1} (van Beek et al., 2011) or 1 month at 0.5 m s^{-1} (Hanasaki et al., 2006). In those models, the distances range is defined from 250 to 1,300 km. The demand points located in the service area of multiple dams use the available water from these dams using proportionality rules. Dams and demand networks are not operated as a system in those studies, as a consequence, a demand may be left unsatisfied even when there is water in other reservoirs upstream but outside the dam service extent. The representation of connections between dams and demand locations is also too simplistic, as topographical barriers which could hinder the adduction of water aren't taken into account. This shows the need to build a more realistic description of adduction networks, and to design water extraction rules which respond to the current state of water resources and demands and can trigger releases from reservoirs managed as a system.

The human water management has to be incorporated into the routing processes at a consistent spatial resolution in order to preserve hydrological continuity. High-resolution topographic information (e.g., 30, 90, and 1 km) are available, but the resolution of atmospheric variables are always coarser for large-scale implementations. In general, routing models will force all runoff generated within a grid to flow in one single direction. In reality, most larger surfaces on land will generate flows in many directions and that needs to be represented by fluxes into many neighboring grid boxes (Guimberteau, Drapeau, et al., 2012). Nguyen-Quang et al. (2018) introduced the concept of hydrological transfer units (HTU) in the routing module of ORganizing Carbon and Hydrology In Dynamic EcosystEms (ORCHIDEE) (de Rosnay et al., 2003; Ducoudré et al., 1993) to bridge the gap between the atmospheric and hydrological processes resolutions. Other LSMs have used similar approaches (Chaney et al., 2016). The basic HTU represents sub-grid river basins and their hydrological connection so runoff generated in one atmospheric cell can flow into multiple neighboring grid boxes. These smaller units allow to better represent the natural river systems and thus facilitate the placement of human water infrastructures as we describe below.

In this study, we aim to develop ORCHIDEE by incorporating human water management using the HTU methodology (Nguyen-Quang et al., 2018) to access needed hydrological information at a higher spatial resolution. The new model is designed to precisely specify the irrigation area, the dams location, the river networks and the water supply demand links. The strategies of water extraction, demand propagation and dam regulation are embedded in the routing module to ensure hydrological continuity. The human water management directly changes the river discharge and in return it will exert feedbacks onto the land surface processes (e.g., soil moisture, evaporation, and runoff generation). Because of high computational cost, the

development of the human water management parametrization for a LSM (i.e., ORCHIDEE) is executed in an off-line version of the model and only over a continental scale catchments, the Yellow river basin (YRB). This study will thus focus on the impact of human water management on river discharge, which can be solved by separating out the routing processes and human water management module from the rest of the LSM. To illustrate the modeling, the impacts of irrigation and dams regulation on river discharge are assessed in their temporal and spatial distribution over our test region.

The overall descriptions of the new model are included in Section 2 and some details are supplemented in the Appendix. The definition of river networks which allows to simulate the flow of water and upstream propagation of demands are introduced in Section 2.1. The equations for dams, routing reservoirs and other water bodies are presented in Section 2.2. The human water management information related to the water usage and demand propagation is introduced in Section 2.3. The application of the proposed model to the test region of the Yellow River is analyzed in Section 3. Followed by a discussion of the advantages brought by this novel approach and some longer term perspectives.

2. Methods

2.1. Definition of a River Network Which Includes Human Activities

LSMs have had sub-grid representations of land processes for decades but in all cases these tiles were statistically distributed and with the only relation between them being that they belong to the same atmospheric grid. Here we introduce a parametrization of sub-grid processes which respects the hydrological connectivity of the sub-grid elements (HTUs) (Nguyen-Quang et al., 2018). This becomes important when the irrigation demands calculated on the atmospheric grid (which are driven by the atmospheric evaporative demand and vegetation states) are linked with the water stores in the river network as it integrates the natural hierarchy of water availability. HTUs are groups of 1 km pixels flowing to the same downstream HTU. Human water management, including the irrigation demand, water supply from rivers and dams will be dealt with at the HTU level. These developments are conceived so that they can be integrated into the ORCHIDEE LSM.

This section introduces the river routing and adduction networks, which defines the direction of water flows and water demand propagations upstream. The adduction connects the water supply and the water use ends. The adduction connections will be built using least-cost functions. The demand propagation network will be the converse graph of the water flow.

2.1.1. Graphs of Water Flow and Demand Propagation Flow

The river routing network is derived from the routing one used in the ORCHIDEE LSM (Nguyen-Quang et al., 2018). In order to simplify the description of the model, we first reinterpret its concepts using graph theory. It not only simplifies the presentation of the method but also facilitates the implementation of supply/demand approaches to human water management.

The water flow is defined on a forest of directional rooted tree graphs (Foulds, 1992) (see Figure 1a). Each tree represents a river system and is described by $D = (V, E)$ where V are the vertices, and E are the edges that connect the vertices. The HTUs in ORCHIDEE correspond to the river system vertices. Each tree has a root which is either located at the coast (the river mouth) or a lake when we deal with an endorheic basin.

In ORCHIDEE's implementation, each vertex (and thus HTU) is fully contained in one grid box (defined as the atmospheric forcing and the same in ORCHIDEE). The grid of ORCHIDEE can contain more than one vertex of the routing graph and can be traversed by more than one graph. Each vertex contains three water stores, characterized by their time constants (slow aquifer, fast aquifer, and stream storages). The properties of these stores are defined by the local slope and tortuosity of the river segment represented by the downstream edges. This governs the residence times of the water in this HTU and thus governs the flow along the edge toward the downstream HTU.

A sample segment of a river graph is shown in Figure 1a. Adduction system for irrigation will generate secondary edges for the vertices. As illustrated in Figure 1a with red edges, vertices within one tree can

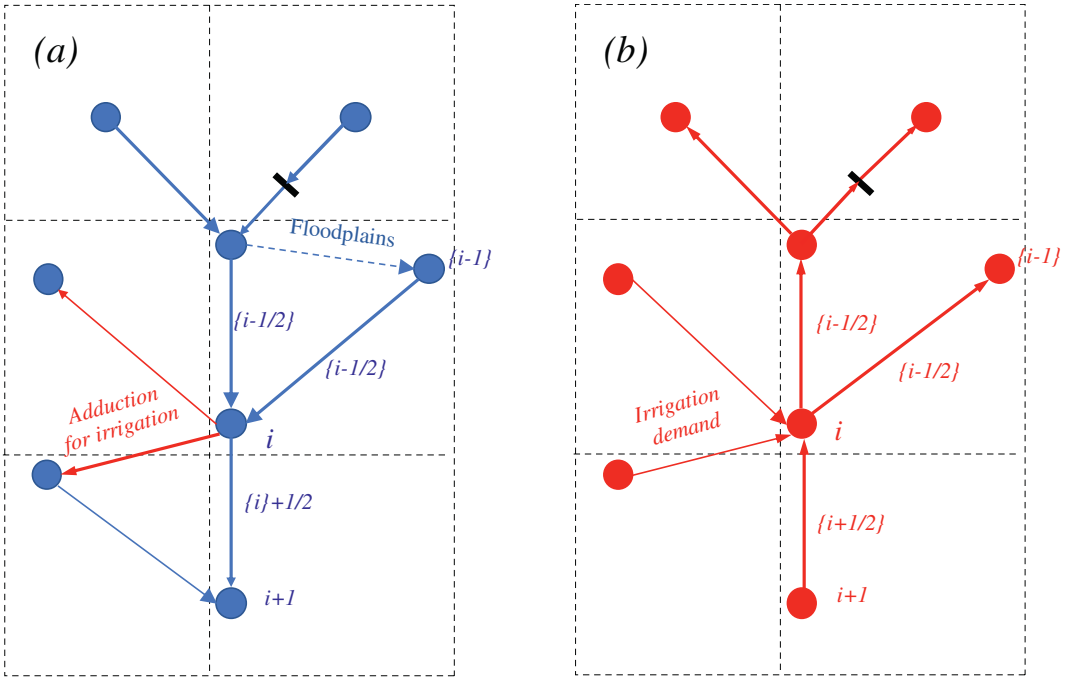

Figure 1. (a) Graph of water flow and (b) Graph of demand flow in the river network. The indexing convention is also presented on the graph with integers used for vertices and half indices for edges. The dash lines represent the grid of the atmospheric forcing used by ORCHIDEE. There can be multiple HTUs in one grid box. Each circle represents one HTU in ORCHIDEE. Dams are symbolized by black bars and located on edges. Their control is based on information from the upstream and downstream vertices. $i + \frac{1}{2}$ indicates the outflow edges from HTU i while $\{i - \frac{1}{2}\}$ represents the ensemble of inflow edges into HTU i. HTUs, hydrological transfer units; ORCHIDEE, ORganizing Carbon and Hydrology In Dynamic EcosystEms.

share water with an adjacent tree through the adduction network and thus allows inter-basin transfers. The methodology for defining this adduction network is discussed below.

The model contains a second directed rooted tree graph (Figure 1b) for the propagation of water demands. This is converse graph (D') allows to propagate the water demand for human usages upstream, that is away from the root of the graph. The flow of information is essential to formulate water management rules and parametrize release functions from coordinated dams systems. As, this is a simpler tree there is no ambiguity on its acyclicity.

The indexing convention used here for the river/demand graph is presented in Appendix A.

2.1.2. Definition of the Adjacency Matrices

The forest of trees, that is the ensemble of connectivity of all river systems, has to be established in ORCHIDEE for a given atmospheric grid. The result which provides the connectivity between all the HTUs defined in ORCHIDEE is called the adjacency matrix. This is performed in three steps: The graph of natural river flow and position of dams, the water demand locations (irrigation here), and finally the water supply demand links.

2.1.2.1. The River Graph

The natural river flow graph is established through a simplification of the HydroSHEDS (Lehner et al., 2008) network on the grid of the model using a super-meshing technique (Farrell et al., 2009). HydroSHEDS provides detailed information, including the flow accumulation, flow direction, elevation, of each high-resolution (1 km) pixel. However, the 1 km pixels are too detailed for the typical spatial resolution LSMs use when driven by global or regional atmospheric models. When the water fluxes exchanged with the atmosphere are simulated at resolutions ranging from a few to hundreds of kilometers there is not enough information

to reasonably feed a horizontal transport scheme at a 1 km resolution. Thus, the ORCHIDEE model groups the fine grid cells with the same general flow direction into basic units of the routing which are called HTU as described previously. The strategy to define the HTUs is based on the Pfafstetter system (Verdin & Verdin, 1999) and the procedures for aggregating the high-resolution information are described in Nguyen-Quang et al. (2018). A criterion of the maximum area of each HTU and a maximum number of the HTUs in each cell of the grid are prescribed by the user to control the size distribution in the HTU space. Each HTU is a vertex of the graph and is represented by a blue circle in Figure 1.

2.1.2.2. Dam Locations

Dams are located in the HTU graph according to their geo-referenced information. The Global Reservoirs and Dams (GRanD) database provides for each of the 6,872 selected dams the coordinates of the dam and the upstream area (Lehner et al., 2011). The coordinates alone are not sufficient to locate the dam on HydroSHEDS as the upstream area of the infrastructure also needs to be correct. To place the dam on the HydroHEDS grid, the location is moved from its initial coordinates downstream following flow direction until the difference of upstream area between HydroSHEDS and GRanD is minimal. Should the upstream area be larger in HydroSHEDS than GRanD, no attempt is made to correct as many upstream locations could exist which minimize the error. This procedure allows to ensure that the infrastructures provided by the database are consistent with the river graph.

During the HTU construction process, the existence of a dam on the 1 km pixel determines if the vertex and some upstream vertices are considered as reservoirs managed by the dam or not. The release from this reservoir will then be controlled by the downstream demands and water stored (see Appendix B2). Each dam is placed on an edge of the graph and is represented by a small black rectangle in Figure 1.

2.1.2.3. Irrigation Points

The fraction of areas equipped for irrigation also needs to be distributed over the different HTUs. However, the map used here is the gridded fraction of potentially irrigated area from the FAO at 10 km spatial resolution (Siebert et al. 2013). With the minimization of the Cost function (Equation 2), we downscale to the HydroSHEDS using the assumption that the easier the access to water is the higher the probability to find a pixel equipped for irrigation. Thus we assign the irrigation fraction to pixels with the lowest Cost first, until the total fraction of irrigation area provided by the FAO map is reached. During the HTU aggregation process, the 1 km pixels are summed up to estimate an irrigation area at the HTU level.

2.1.2.4. The Adduction Network

The adduction network setup is inspired by the methodology of Optimal Dam Dimensioning Yield and Climate Change Economic Impact Assessment (Neverre et al., 2016, ODDYCCEIA). It connects the demand locations with the most likely abstraction vertex on the river graph. For irrigation, the location of the demands has been described in the previous paragraph. The strategy to find the adduction path is to minimize a cost function corresponding to the difficulty of transfer from the river to the demand's location.

The original cost function in Neverre et al. (2016) has two terms, one corresponding to the vertical water movement from lower to upper places and the other to the infrastructure needed to transfer water horizontally. This cost function is not an explicit economic cost function but materializes that moving water up and horizontally involves some infrastructure and operation economic costs.

$$\text{Cost} = D^{\text{path}} + k \cdot H^{\text{path}}, \tag{1}$$

where Cost is the total "cost" along the adduction path. D^{path} is the horizontal distance along the path, H^{path} is the cumulative elevation increments along the path. It is always a non-negative value. In general, lifting water is much more difficult than transferring it horizontally, since it requires pumping water or building aqueducts and tunnels. This is taken into account by the k factor which describes the ratio of costs between both directions. It can be constant or it can be made country or even location dependent to take into account differences in wealth, technical capabilities and opportunities to satisfy the demands.

Neverre et al. (2016) propose a two-step approach; The least-cost path described above, obtained using topographic information, is completed by a second step taking into account the average flows on the vertex to

ensure demands can be matched. Here, another approach is proposed to take into account water availability that does not require to know demands and inflows beforehand. We suggest to use the upstream area of the catchment at the abstraction point to favor the links which have the highest likelihood to carry water. In other words, catchment area is considered as a proxy for inflow. This leads to an alternative cost function:

$$\text{Cost} = \frac{D^{\text{path}} + k \cdot H^{\text{path}}}{\log(U)}, \tag{2}$$

where U is the upstream area of the abstraction point. This formulation ensures the unicity of the adduction path to a given river as U is a monotonic function along the graph. The value used here is the same as the one recommended by Neverre et al. (2016) ($k = 10{,}000$).

This methodology to construct the adduction network is applied to the 1 km resolution description of the rivers and links each potential demand point with a point on a river with an upstream area greater than 10,000 km^2 or a dam along the river network. The aggregation to the HTU level then preserves this information and allows to setup the edges between the river HTU and the demands HTU over which water can be transferred. Adduction paths from one HTU to multiple other HTUs are preserved. The demands generated on an HTU are distributed among the multiple water source HTUs according to the density of paths available at 1 km resolution. Resulting multiple adduction path between two HTUs are aggregated as one edge to carry the water transfers and demand information.

2.2. Water Continuity Equations

2.2.1. Definition of Water Stores and Water Classes

Each vertex (HTU) is associated with stores with different properties. Three types of stores are distinguished: The natural unmanaged water stores, the stores created and managed by humans and a special store corresponding to the naturalized flow.

In the model, aquifers are considered to be unmanaged and are represented by two aquifers: a fast aquifer (W_{fast}) and a slow aquifer (W_{slow}). These aquifers correspond mainly to alluvial/shallow aquifers. They differ in their time constant which describes the recession rate for each water storage (see Equation 3). With a very large time constant for the slow aquifer, the water stored in the slow aquifer can be extracted as the shallow (or renewable) groundwater. These two aquifers can feed irrigation through water pumping. These sources are purely local to the HTU because they are only fed by the runoff and drainage from the current grid.

The surface water can be affected by human usage. Different classes are defined and indexed by k:

- Natural river flow: $k = 0$
- Ecological and non-reserved flow: $k = 1$
- Domestic and industry: $k = 2$
- Irrigation: $k = 3$
- Hydro-power: $k = 4$

$k = 0$ is the natural potential for the river system and corresponds to a river system without any human interventions. This flow can be compared to naturalized discharge data provided by some basin agencies. It is also used here as a reference for the rules of some managed classes.

By separating the water in the streams into four managed classes ($k = \{1...4\}$), the model can follow the type of demand water was released for. It is akin to a storage of water in the streams and helps to formulate management rules. By default all the water is "ecological and non-reserved flow" but operational rules can transfer some of the stream flow into other classes. Note that the class index is also a priority parameter that is used when releasing from the dams. The priority decreases with increasing index. Note that the fast aquifer and slow aquifer only have two water class $k = 0$ and $k = 1$, representing the natural (without human interventions) and altered status (with human interventions).

2.2.2. Prognostic Equations for the Stream Store

The continuity equation for the water flowing has been reformulated due to additional water classes and the addition of lakes and man-made reservoirs (See Appendix B).

2.2.2.1. River flow

The outflow flux from the three water storages *Fs* (stream, fast, and slow) for HTU *i* and the class *k* is given by

$$Fs_{i+\frac{1}{2},k} = \frac{W_{X,i,k}}{g_X \cdot \tau_i}, \tag{3}$$

W_X is the W_{stream}, W_{fast} or W_{slow} representing the water storage in the river water storage, fast aquifer, and slow aquifer, respectively. $i+\frac{1}{2}$ indicates the outflow from HTU i (in reverse, $i-\frac{1}{2}$ represents the inflow into the HTU i). The fluxes are determined by the following properties which are either HTU dependent or constant in space and have been described in previous publications using ORCHIDEE's routing scheme (d'Orgeval et al., 2008; Ngo-Duc et al., 2007; Nguyen-Quang et al., 2018). g_X is the g_1, g_2, and g_3 for the three storages.

- g_1: Time constant of river water storage in unit day km^{-1}
- g_2: Time constant of fast aquifer in unit day km^{-1}
- g_3: Time constant of slow aquifer in unit day km^{-1}
- τ_i: Topographic index for each HTU i in unit m^2

The fluxes from the fast or slow aquifers will be added to the river water storage of the downstream HTU.

2.2.2.2. Water Bodies (Lakes and Reservoirs)

The information of the water bodies is derived from the Global Reservoirs and Dams Database (Lehner et al., 2011, GRanD). If the water body ends with a dam, the water body is considered to be managed, else the water body is considered a natural lake. In the case of a natural lake the water above the capacity will flow out with a given time constant:

$$Re_{i+\frac{1}{2},1} = \max\left(\frac{V_i - Vref_i}{g_4}, 0\right) \tag{4}$$

$$Re_{i+\frac{1}{2},2\ldots4} = 0 \tag{5}$$

$Re_{i+\frac{1}{2},k}$ is the outflow from HTU i with the water class k. V_i is the current water volume stored in the lake i. $Vref_i$ is the reference water storage, defined as the maximum water storage below the lake outlet. g_4 is the time constant of the water in the lake (unit: day km^{-1}). We propose to set it equal to time constant of the slow aquifer for the moment (g_3). Note that the lakes will not serve as the water sources for demand categories other than the ecological and non-reserved flow ($k = 1$).

If the water body is controlled by a dam the demands drive the release. Some volume is also reserved, using a one point hedging rule with the hedging coefficient $\alpha_{i,k}$ (Draper & Lund, 2004), which can be specific for each water class. The releases are computed for each class and then subtracted from the river water storage $W_{\text{stream},i,k}$ and thus the total stored volume V_i.

$$k = 1 : Re_{i+\frac{1}{2},k} = \min(\alpha_{i,k} V_i, \max(d_{i+\frac{1}{2},k}, V_i - Vref_i)) \tag{6}$$

$$k = 2\ldots4 : Re_{i+\frac{1}{2},k} = \min\left(\alpha_{i,k}\left(V_i - \sum_{\kappa=1}^{k-1} Re_{i+\frac{1}{2},\kappa}\right), d_{i+\frac{1}{2},k}\right) \tag{7}$$

V_i is the current water volume stored in the reservoir i and $Vref_i$ its known storage capacity. The varying $Vref_i$ is defined in the next subsection. $d_{i+\frac{1}{2},k}$ is the downstream demand in value class k and it is unique as it is part of a directed graph. The ecological and non-reserved flow also includes the spill from the dam, the release of water above $Vref_i$. $\alpha_{i,k}$ is the hedging coefficient which tries to anticipate the future dynamics of the demands ($\alpha_{i,k} \leq 1$).

This methodology ensures that ecological flow ($k = 1$) is given priority. The other demands are satisfied as long as water volume is sufficient, taking into account hedging. For a demand with index k, the summation of other demands up to $k - 1$ ensures that the demands with the highest priority (lower index) are served first. Hedging, increases the risk of spill but allows to keep water stored, which can be used later, such that demands with higher priority can be better served.

2.2.2.3. Hydro-Power and Flood Management

In the flooding season, the maximum storage of the dam is reduced to a lower level to ensure that enough capacity is available to absorb potential floods without exceeding the design limits of the infrastructure. Outside of the flooding season, the maximum dam storage is set to the maximum level that is safe for the dam, in order to store as much water as possible for demands satisfaction, and also in order to produce hydro-power in the best conditions. The upper limit of water level is therefore varying with time as shown in Figure S1. This information is not provided in the dam information of GRanD (Lehner et al., 2011) but can be derived from the climatology of the simulated natural discharge by the model or obtained from the literature. In this first implementation, flooding volumes are based on local information on flood volume rules.

In the water management scheme proposed here, hydro-power water demand is not explicitly taken into account. There are no releases targeted at satisfying exclusively hydro-power water demand. The water for hydro-power is not consumptive thus any release can actually be used for hydro-power. Although this assumption means that some hydro-power demand is ignored, it also ensures that the reservoir level only decreases when higher priority demands need to be satisfied. This is consistent with keeping the reservoirs at the highest possible level to maximize the energy production for a given water release.

2.3. Flow of Water Demands

2.3.1. Definition of Demands

The water demands for the various water classes are one of the key information which allow to derive management rules for reservoirs and extraction functions from the streams. We define three variables to store and propagate this information. First, there is the local demand on each vertex $dl_{i,k}$ which represents the water needs for use k that should be withdrawn from vertex i. For irrigation for instance, it is the sum of the needs which are fed through adduction channels to this point in the river graph. The irrigation demand can, therefore, come from an area larger than the grid box containing the current vertex. The second information is the unsatisfied demand $du_{i,k}$ which results from the local demands which could not be satisfied with the water currently in the stream store. This information needs to be propagated upstream to trigger releases from reservoirs. Finally, the third demand is the sum per value class of all the downstream demands $d_{i+\frac{1}{2},k}$, which allows to decide if an abstraction should be performed to satisfy a demand. As this information is akin to a flux it is placed on the edges of the graph. It is used to define the water releases of the reservoir in vertex i (Equations 6 and 7) as an argument to the release function $Re_{i+\frac{1}{2},k}$. In the following section, we describe the equations used to compute and propagate this information.

To facilitate the expression of the prognostic equations for the stream reservoirs (Equation B1) an extraction term is also defined as $e_{i,k}$, or $e^{1}_{i,k}$ when it is transferred to the unallocated water. It is directly given by the difference between the local demand and its unsatisfied part. Its calculation is detailed in Appendix C together with the definition of the demands.

2.3.2. Unsatisfied Downstream Demands

Unsatisfied water demands are generated at each consumption point within the graph. It will propagate along the digraph defined in Figure 1b and be used in HTU where water is managed to compute releases. By definition, at the root of this digraph (the river outflow point) the unsatisfied demand is zero.

Each HTU will have an unsatisfied demand $du_{i,k}$ when the water needed for irrigation, hydro-power, domestic use and ecological flows is not available locally. This information needs to be summed with the downstream unsatisfied demand so that at each vertex, where water management infrastructures exist, a total downstream demand $d_{i+\frac{1}{2},k}$ is available to compute releases and apply operating rules.

This is achieved by writing a continuity equation for the demands. The continuity equation can be written for the sum of all upstream demands:

$$\sum_{m\in\left\{i-\frac{1}{2}\right\}} d_{m,k} = du_{i,k} + (d_{i+\frac{1}{2},k} - Re_{i+\frac{1}{2},k}), \tag{8}$$

where $Re_{i+\frac{1}{2},k}$ is the water released by the infrastructure at vertex i (See Appendix B2). $m \in \{i-\frac{1}{2}\}$ denotes all the upstream HTUs flowing to HTU i. $du_{i,k}$ is the unsatisfied water demand at HTU i in water class k. $d_{i+\frac{1}{2},k}$ is the total downstream water demand at HTU i in water class k.

However, we want to propagate this demand along each of the upstream edges in order to reach each of the upstream dams until the demand is satisfied. An algorithm is needed in order to distribute this overall downstream demand over upstream edges. As proposed by Neverre et al. (2016) we distribute the demand as a function of the stored water in each of the upstream basins. To achieve this, we use the information of the water currently stored in all upstream reservoirs Vu_i. The continuity equation for the demands thus becomes:

$$d_{i-\frac{1}{2},k} = \frac{Vu_{i-1}}{\sum_{m\in\{i-1\}} Vu_m}\left(du_{i,k} + d_{i+\frac{1}{2},k} - Re_{i+\frac{1}{2},k}\right). \tag{9}$$

$\{i-1\}$ denotes the ensemble upstream tributaries which have their confluence at HTU i. The downstream demands are distributed upstream proportionally to the total storage in each tributary. Another simpler option would be to distribute demands according to the installed storage capacity irrespective of their current status. In that case in the above equation Vu_{i-1} would be replaced by the total upstream storage capacity $Vuref_{i-1}$. More complex options could also be used, such as the space rule (Johnson et al., 1991) or rules parametrized by optimization (Nalbantis & Koutsoyiannis, 1997).

2.3.3. Sequence of Water Sources

Demands will first be satisfied with water in the streams and then from the fast and slow aquifers of the same HTU. As these two aquifers have large time constants, extraction from them can be considered as shallow groundwater pumping. The unsatisfied demand will then extract water from the river HTUs linked to the demand through the supply demand path. The remaining unsatisfied demands will then be propagated to the upstream dams for water release with Equation 7. Note that the propagation (Equation 9) needs to be solved starting at the outlet of the rivers to provide at each point of the graph the cumulated demand to which the management infrastructure will need to respond with releases.

Currently ORCHIDEE does not include fossil groundwater (non-renewable groundwater). Therefore, irrigation demands cannot be satisfied with pumping from deep groundwater as is the case in some regions of the world. However, this does not impact the objective of our study as we focus on the impact of human water management (including irrigation, dam regulation) on river discharge. Compare to surface water, fossil groundwater is only a small proportion of the water used in this region for irrigation (Wada et al., 2012). Furthermore, most of it will be consumed by evaporation and thus its impact on the river flow should be negligible.

2.4. Implementation of the Model

The proposed model for human water management has been implemented in ORCHIDEE's routing module. Given the high computation requirement, the LSM was run uncoupled from its routing module to simulate the water inputs (runoff and drainage) which drive lateral transports of water and irrigation demands. Simulating the rivers without the LSM facilitates and speeds-up development, but has implications. The main implication is that we assume for the purpose of this study that all the water abstracted for irrigation reaches the atmosphere and that the return to the river is negligible. In other words, agricultural demand is assumed to be fully consumptive here. Once the routing scheme is integrated into ORCHIDEE this assumption will not be needed any more as the irrigated water not used by the plants will leave soil moisture through drainage and return to the rivers.

The water required for irrigation is also estimated in the LSM and used as a demand for the proposed human water management model. The agricultural demand is estimated as the deficit between the actual and potential evapotranspiration computed by ORCHIDEE for the grid, as described in Guimberteau, Laval, et al. (2012) and Yin et al. (2020). Precipitation (P) and reinfilterating surface runoff (Re_{inf}) are subtracted from the unfulfilled evapotranspiration (calculated as difference between the potential evapotranspiration [PET] and actual evapotranspiration [ET]) in order to estimate the irrigation demand (d'Orgeval et al., 2008).

$$d = \max\{PET - ET - (P + Re_{inf}), 0\} \tag{10}$$

The agricultural demand is estimated on the 0.5° grid as this is the resolution at which the atmospheric variables are available. It is then distributed to the 1 km pixels by the percentage of the irrigation area at the HTU level as described in Section 2.1.2. Note that in ORCHIDEE, the estimation of the irrigation demands is more complex as it considers explicitly the transpiration's soil moisture stress thus taking into account the state of the vegetation when the dry spell arrives (Guimberteau, Laval, et al., 2012) and it is only applied to the crop fraction of the grid. The updated irrigation module, including flood and paddy irrigation technologies, was developed in the ORCHIDEE-CROP LSM which describes crop phenology and growth (Yin et al., 2020). The simulations have been validated with observations and census data over China from 1982 to 2014.

To estimate the runoff and drainage needed for the routing module, ORCHIDEE was driven by the WFDEI_CMA forcing. This data set is the WATCH Forcing Data (WFDEI) based on the ERA-Interim reanalysis data in which the precipitation estimates from China Meteorological Association (CMA) were used to correct the re-analysis (Zhou et al., 2018). The spatial resolution of the atmospheric variables is 0.5° and the temporal interval is 3 h. The simulation was executed with a time step of 15 min to account for fast exchanges within the continental hydrological water cycle.

Three scenarios (natural: NAT, irrigated: IRR, regulated: REG) are designed to evaluate the impact of human water management on river discharge. NAT represents natural conditions, that is without considering irrigation or dam regulation. IRR represents a situation where irrigation exists but the river is not regulated. Both irrigation and dam regulation are activated in the simulation REG. The differences between NAT and IRR allows to evaluate the impact of irrigation while the difference between IRR and REG shows the contribution of dam regulation to the potential for irrigation under current climate condition. The comparisons between NAT and REG shows the combined impact of the human water use and management (irrigation and dam regulation).

3. Test Implementation of the Management Scheme

3.1. Description of the Human Pressure in the YRB

The Yellow River is the second-longest river in China, with the main channel of more than 5,000 km in length and a catchment area of 7.5×10^5 km^2. The Yellow River originates on the North Tibet Plateau, flowing through floodplains in the upstream, hilly terrain and the Loss Plateau in the middle section, flat plains in the final reaches before the river flows into the Bohai Sea (Figure 2). It has fed the Chinese civilization for thousands of years and still plays an important role nowadays for agricultural and social development over the YRB. The population over the entire YRB exceeds 100 million in 2017, and will reach 126 million in

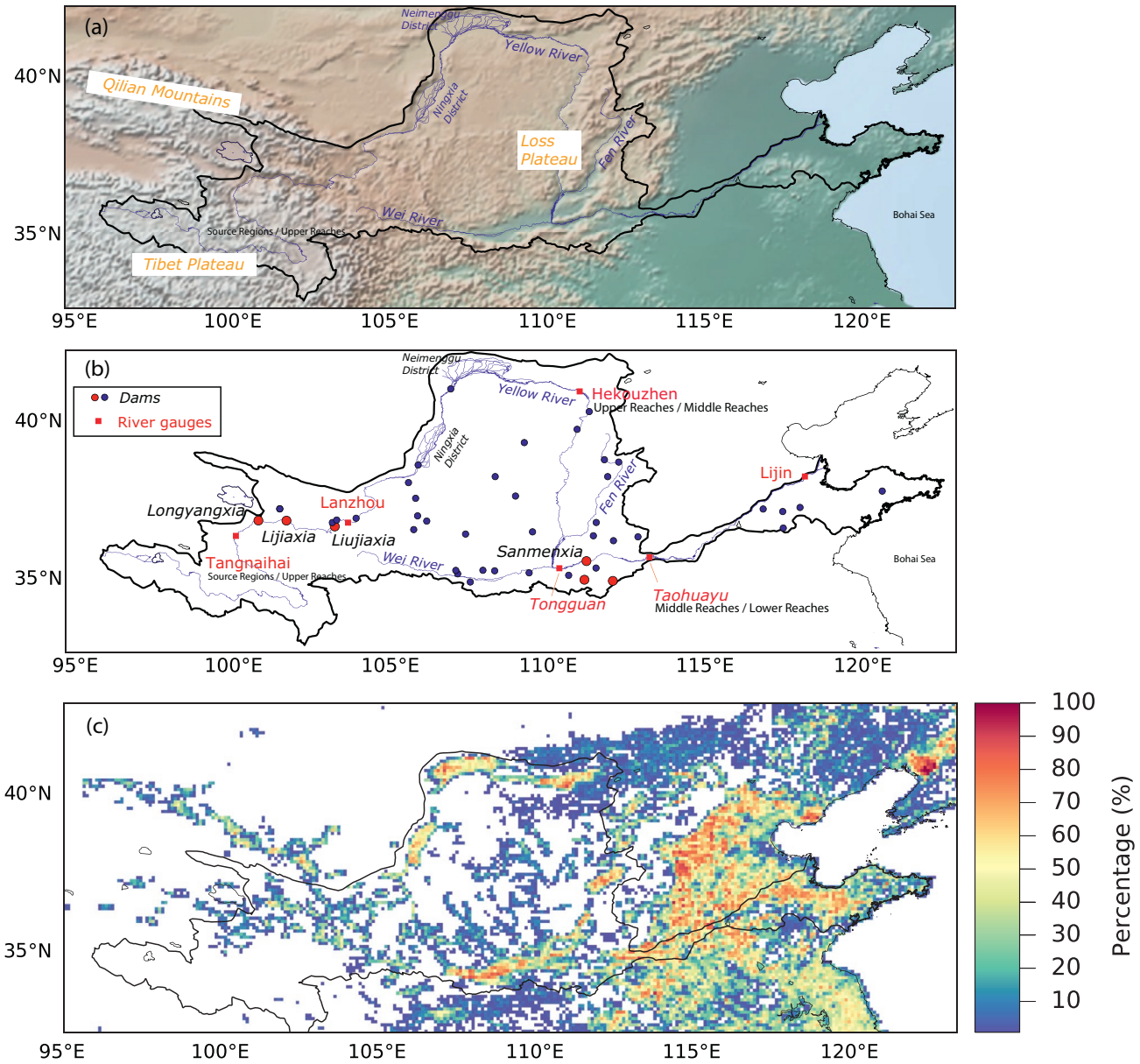

Figure 2. (a) Geography map and (b) detailed locations of the dams and river gauges in the Yellow River Basin. (c) Percentage of irrigated area in Northern China (Siebert et al., 2013). The dams collected in the GRanD database and discharge gauging stations on the Yellow River basin are displayed. The dams with reservoirs larger than 10^8 m^3 are marked with red dots while others are marked with blue dots. The region upstream of the Tangnaihai station is considered as the source region where human interventions are negligible. Hekouzhen separates the upper reaches and middle reaches. Taohuayu separates the middle reaches and the lower reaches. Tongguan is the confluences of the main Yellow River channel with its largest tributaries: Wei and Fen rivers.

2020 (Wang et al., 2018). The cropland area occupies around 2×10^5 km^2, with varying proportion between 26% and 28% of the total catchment area (Wang et al., 2017). The large demand from the domestic and agricultural sectors rely heavily on the surface water resources in the Yellow River as well as the groundwater storage. The Water Resources Bulletins in 2000 (MWR, 2001) reports that about 35% of the total water consumption is taken from groundwater while this proportion decreased to 20.6% in 2019 (MWR, 2020). But there is no information on the fraction which is taken from non-renewable groundwater.

Water resources are scarce in the YRB as large portions of the basin are located in a semi-arid climate and receives annual average precipitation of around 450 mm $year^{-1}$. Together with glacier melt from the Tibet, more than 70% of the surface water in YRB is generated in the upper reaches (MWR, 2020). Large irrigated area, distributed in the upper reaches, consume the discharge along the main river channel. There is a very

little supplement in the middle and lower reaches. Thus despite the presences of the river, the middle and lower reaches rely on groundwater pumping.

To meet the high demand for agriculture, ensuring water availability during the crop growth cycle, and for flood control dams have been built in the YRB. For flood control some space is left in the reservoirs during summer, the high precipitations season. We do not have a precise description of water management rules targeting water uses satisfaction, but it is common knowledge that the operating rules follow the general patterns of filling during the low demand period of winter, and releasing when irrigation demands are high in summer. Allowing a better satisfaction of demands and lowering the water level in the river in the season where floods are more likely.

The Global Reservoir and Dams (GRanD) database reports 49 dams over YRB with 9 of them located along the mainstream. The dams have significantly altered the river discharge in magnitude and phasing. Other information sources for the region shows that additional dams exist, but they are either small or have been completed since the global database was assembled. Taking into account the human activities (e.g., irrigation and dam regulation) is a necessary step to accurately represent the river discharge over the Yellow River and in order to explore the potential interactions of climate change and water management.

There are a number of gauging stations along the Yellow River where observed monthly river discharge are available (Figure 2b). Moreover, the second and most recent national water resources survey provides the naturalized river discharge in which the impact of consumed water and flows modifications by dams have been removed (Zhou et al., 2020). The naturalized river discharge is a useful data source to validate the simulated natural state of the river and the statistics provided by local water management agencies are arguably the most reliable source of information for the actual water management. Given that the naturalized and observed river discharge data spans the periods over 1950–2000 and the model's forcing WFDEI_CMA data is only available after 1979, the period for model simulations is narrowed down to 1979–2000.

3.2. Other Regional Model Settings

In the present implementation, the dam regulation is simplified by selecting a hedging coefficient equal to 1 for all water classes ($\alpha_{i,k} = 1$). Although the flooding period changes slightly along the Yellow River, we have chosen for all dams the period from May 1 to the end of August for the reduced maximum storage to absorb any flood wave. The reduced maximum storage for each dam is calculated as a percentage of its nominal capacity. The ratio is obtained from available data for the dams in the Yellow River. A simple regression has shown that 60% is the common reduction rate for the region. Dams start to refill this flood buffer in September at a limited maximum rate until the reservoir reaches its nominal capacity. Dams start to release water from January 1st the following year to lower again maximum storage. This release of stored water is also limited to a maximum rate. The maximum spill and fill rates are obtained by dividing the change in volume between $V_{\max}$ and v_{flood} by the time foreseen for the operation.

In order to simplify the analysis and also because ecological flows have not been strongly enforced in the Yellow River Basin so far, we have, in this implementation, selected to set the ecological flow to 0 $m^3 s^{-1}$ throughout the year. Since the hydropower demand is non-consumptive and domestic and industrial water demands are mostly non-consumptive, they are not taken into account for testing the new routing model in the YRB.

The analysis of the simulated impact of human water management on river discharge is based on the multi-annual mean values (1979–2000). Although the simulation contains higher-resolution information for routing, water use and water management, the analysis is performed on the coarser atmospheric grid by using the representative discharge value (the HTU with the largest discharge) for a simpler visualization of the results.

4. Results

4.1. Irrigation Distribution and Demand-Supply Paths

The map of the water abstraction cost function (Equation 2) estimated by the algorithm provided in Subsection 2.1.2 is displayed in Figure S2a. The cost function is tightly linked to the topography with high values

found in mountainous areas (Figure S2b). The distribution of low cost areas follows the river channels showing the easy accessibility in the riparian zone. The values of the cost function are also low in the North China Plain as in this sedimentary region there is no penalty for lifting water over topography.

The refined 1 km-resolution map of areas equipped for irrigation derived from the FAO map (Figure 2c) with the methodology presented in Section 2.1.2 is shown as Figure S3b. Both the FAO fraction map and the downscaled high-resolution irrigation points match well with the officially released main crop districts (NPC, 2011). The cropland identified in the land cover map (Figure S4) is generally consistent with the irrigation map although the distinction between rainfed and irrigated croplands is less reliable in the land cover map. This can have two causes, first, the FAO map identifies potentially irrigated areas and second the difficulty to distinguish from space irrigated and rainfed cropland. The consistency of the resulting distribution of irrigation points with the released report (NPC, 2011) and with the total cropland area derived from satellite-based observations gives us confidence in the locations of water consumption. High concentrations of irrigation areas are found in the Ningxia district, the Neimenggu Irrigation district, the lower Weihe River, and the Shandong peninsula. The main concentrations are located in the riparian plain of the Yellow River, corresponding to the areas with the low values of the "cost" function. This is consistent with accessibility to water being correlated with and a determinant of the distribution of irrigated areas.

The connections between a potentially irrigated area on the 1 km resolution map (demand end) and abstraction point on the river (supply end) is constructed by minimizing the cost function displayed in Figure S2a as explained in Section 2.1.2. The resulting adduction network is displayed in Figure 3 by symbolizing each connection with a green line. The average distance of the adduction network is 17.7 km, with a standard deviation of 12.1 km. The distance is shortest in regions with higher density river network and longer in the upper reaches where access to water is more difficult. The adduction network density is high in regions where the "cost" is low, which means that the cost used is a relevant proxy. The average length in the adduction network is smaller than the grid resolutions usually used in large-scale models (e.g., 0.25°, 0.5° or 1.0°) demonstrating the added value of the approach proposed here. The strong inhomogeneity and anisotropy of the network simulated here show that previous approaches which ignore topography will miss some important characteristics of the water transport infrastructures. In general, the irrigation points are connected to the closest river channel, independently of their atmospheric grid box as the network is based on the original 1 km data set, before aggregation into HTUs. Thus the structure of the simulated river network follows more closely the hydrological network and the topography and the adduction network is not significantly constrained by the 0.5° grid.

Some relatively long distance adduction network links are probably spurious. To avoid those links a threshold on the cost could be used, or they could also be excluded if they are in a region with small scale reservoirs, abundant renewable groundwater or year-long water sources. Additional artificial adduction paths are possible (e.g., the South-North water transfer project). Users can specify the supply ends and demand ends from the defined HTUs. Though, it is ignored in this implementation because the investigation period is before 2013 when the project started operating.

4.2. Irrigation Water Demand

Irrigation accounts for the largest fraction of water consumption in northern China. The pattern of estimated irrigation demands is shown as Figure 4a. Areas along the main Yellow River channel already have relatively high potential irrigation demands, ranging from 300 to 900 mm $year^{-1}$. Much higher irrigation demands are found in the China Northern Plain (Hai River), with the annual demands exceeding 1,350 mm $year^{-1}$.

Figure 4b shows the ratios of irrigation demand that can be satisfied by local water (i.e., stream storage, fast, and slow aquifers). In the center Loss Plateau, the water demands for irrigation are small and the local water provided by rainfall can be sufficient. However, local waters are not enough for areas along the main Yellow River in the upper stream, in the Wei River and the lower Yellow River and the Northern Plain. The water required for agriculture has thus to be dealt with in the context of the entire upstream catchment. The local grids will extract water from the nearby rivers through the defined supply demand paths. If the river

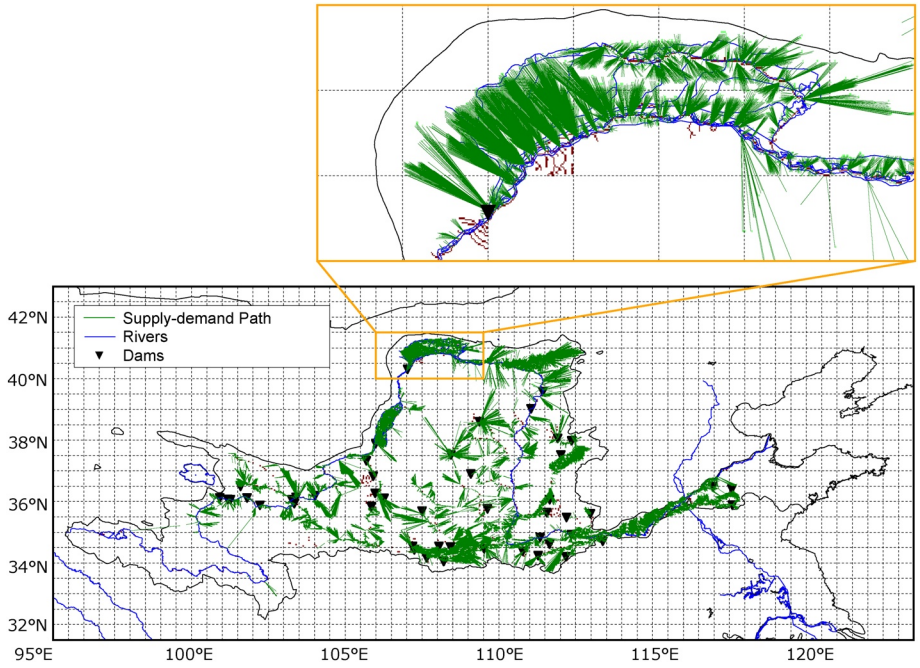

Figure 3. Generated paths (green lines) between the water demand points and water abstraction points, that is defining supply lines. The zoomed map is for the Neimenggu District. The mesh indicates the boundaries of the atmospheric forcing grid used by ORCHIDEE here. ORCHIDEE, ORganizing Carbon and Hydrology In Dynamic EcosystEms.

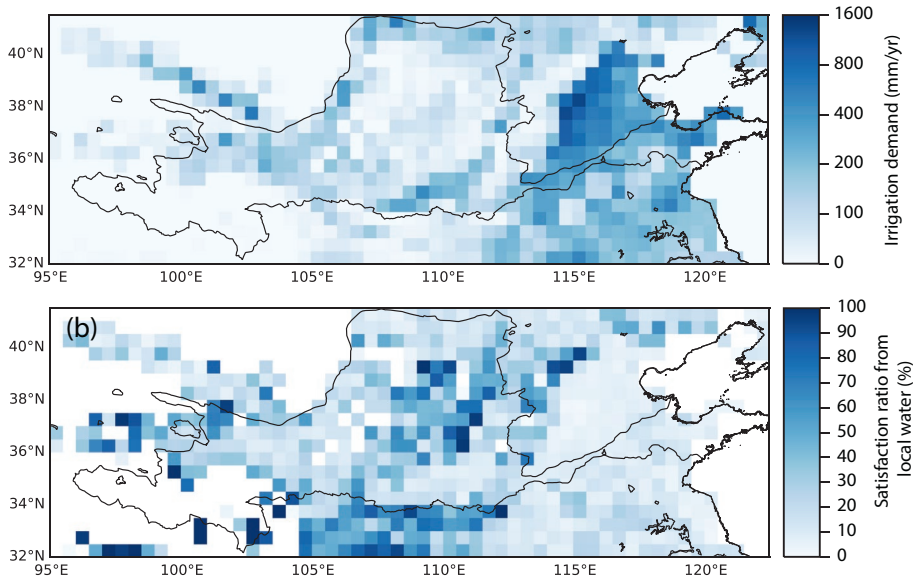

Figure 4. (a) Long term average (1979–2000) total irrigation demands and (b) satisfaction ratio of the demands by local water from river water storage, fast and slow aquifers. The values are shown as the mean over all HTUs on the 0.5° atmospheric grid. HTUs, hydrological transfer units.

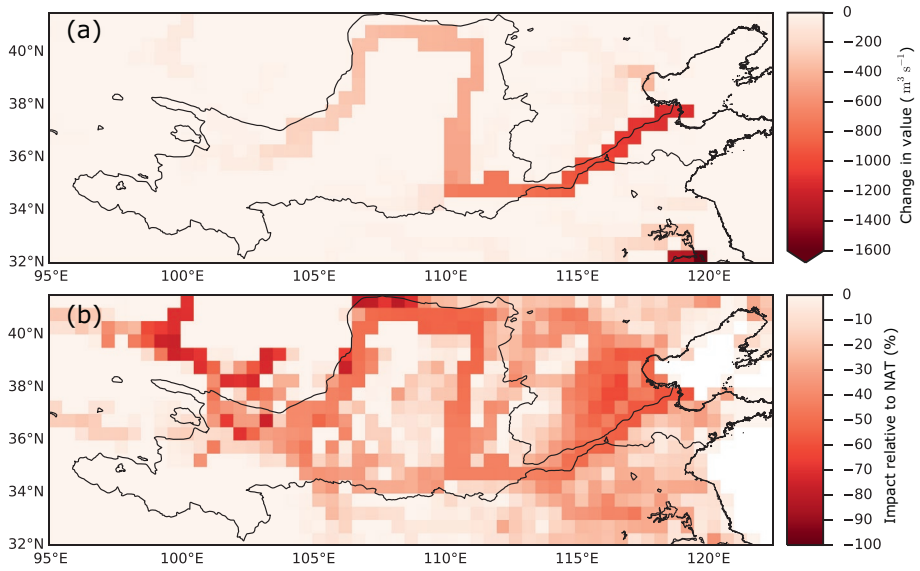

Figure 5. Estimated irrigation impact (IRR-NAT) on river discharge (a) in absolute values and (b) as relative change over the 1979–2000 period. On the atmospheric grid the discharge of the main HTU which flows out of the cell is represented. HTUs, hydrological transfer units; IRR-NAT, irrigated-natural.

water still does not cover the need, the unsatisfied water demand will be propagated upstream. In the IRR scenario, the propagation will not change the results because dams are not included in the IRR scenario.

4.3. Impact of Irrigation on River Discharge

As shown in Figure 5, the total abstraction for irrigation accumulates along the main river channel decreasing the discharge by 1,320 $m^3 s^{-1}$ at the Lijin gauging station. The change relative to the natural state of the river (Figures 5a and 5b) shows an important impact of irrigation not only along the river channels but also in some upper tributaries where water resources are limited. The relative change is small in the source regions of the YRB where human intervention is limited. In contrast, the relative change is high to the north-west of the YRB. Agriculture in that part of the Gansu province relies heavily on irrigation using water which runs off the northern slopes of the Qilian mountains. The northern part of this province is located in the Gobi Desert and thus offers no water resources. In the Neimenggu District, the natural river discharge change reaches −90%, indicating a dramatic decreasing of local river levels caused by a high demand for water from the main Yellow River.

Along the mainstream of the Yellow River, the impact of irrigation starts to increase right after the river flows through the gauging station of Tangnaihai. As the river flows North it goes through densely irrigated areas (Figure 2c). Irrigation impact reaches a peak before the Hekouzhen gauging station (∼ −58.0%, black dots in Figure 6), after the main irrigation district in the Neimenggu province. Then the impact declines progressively as other tributaries less affected by irrigation contribute to the discharge of the Yellow River. The impact of irrigation on the two main tributaries Fen (−34.9%) and Wei (−31.3%) is slightly lower than the main channel (−41.8% before the confluence of the Fen River). The annual mean reduction in the main channel is not modified significantly after the confluence since it is −42.7% right after the merger with the Wei River. The impact in the lower reaches keeps increasing until the estuary of the Yellow River. This evolution of the impact of irrigation on the river discharge is nicely illustrated when plotting it along the main channel as a function of the distance to the ocean as shown in Figure 6. The annual mean change relative to the natural state of the river is shown with black points in this figure.

The impact of abstractions for irrigation differs over the course of the year (see the colored points in Figure 6 for the four seasons). Winter shows the smallest changes because of low energy (heat and radiation) availability and thus reduced irrigation needs. In summer, during the cropping season, the irrigation needs are the highest and the abstractions are also the largest. The impact increases downstream of

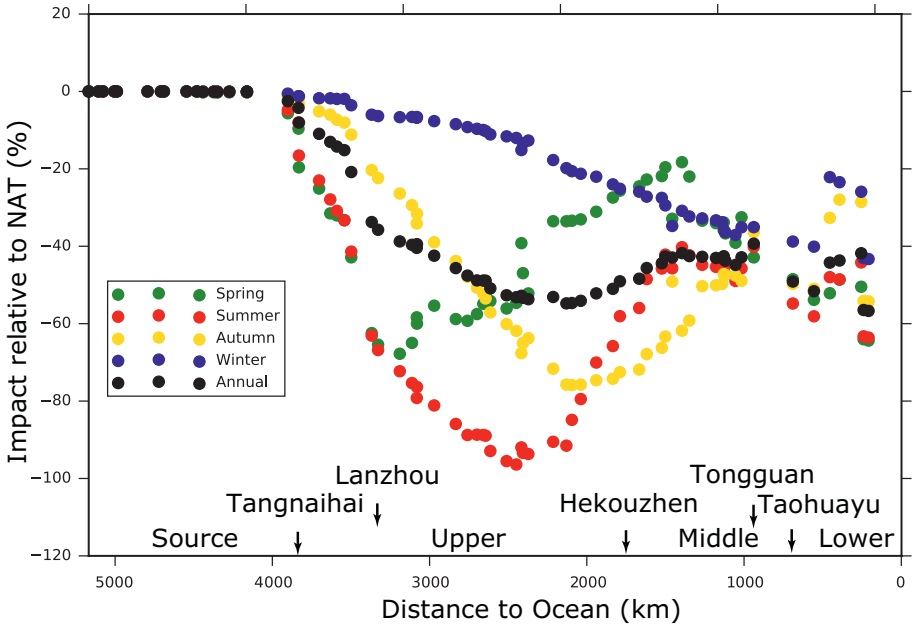

Figure 6. The impact of irrigation relative to the natural discharge of the yellow river along its main channel (IRR-NAT). The long term averages (1979–2000) of annual as well as seasonal flows are displayed. The discrete dots represent the grids along the main river channel. The named stations are positioned on the map in Figure 2. The definitions of the seasons are as follows: Spring covers March to May, Summer June to August, Autumn September to November and winter covers December to February. HTUs, hydrological transfer units.

the source region but at different rates, reaching its maximum impact before the middle reaches in every season but winter.

In spring, the cumulative abstractions are the highest at the Lanzhou gauging station. Then, the impact starts to decrease because of the confluence of small tributaries which carry large amounts of water in the spring season with fewer irrigated areas. When the two main tributaries (the Fen and the Wei river) join the main channel, before the Tongguan gauging station, the impact of irrigation increases again as these rivers are strongly impacted by abstractions during this season (Figure S5). The impact of irrigation is −43.4% and −45.6% for the two tributaries. Correspondingly, the main channel impact of irrigation increases from −18.2% to −33.4% after the confluences. The spatial distribution of IRR-NAT (the difference between IRR and NAT simulations) in the four seasons demonstrates that in the Wei and Fen rivers irrigation discharge decrease is indeed stronger in spring (Figure S5).

In summer the decrease of discharge continues downstream of Lanzhou gauging station because of the large irrigation demands in the irrigation districts of the Neimenggu province. There is again a decrease of the irrigation impact downstream with a less pronounced effect of the Wei and Fen river than in spring. The peak reduction relative to natural flows reaches 95% and occurs closer to the estuary (~2,500 km to the ocean) than in spring. The river section downstream of the Tongguan gauging station is known to be characterized by high water stress which may result in severe water scarcity not only for agriculture but also for domestic and industrial sectors (Cai & Rosegrant, 2004).

In autumn the impact of impoundments for irrigation starts to reduce and the peak occurs downstream of the Neimenggu irrigation district (~2,000 km to the ocean, upstream of the Hekouzhen gauging station). The peak discharge decrease is 80% in autumn, and then the impact decreases to 50.3% where the two main tributaries join.

Because of small irrigation demands in winter, the impact progressively increases from the source regions to the end of the middle reaches. In winter, the impact of abstractions on the discharge of the Wei and Fen

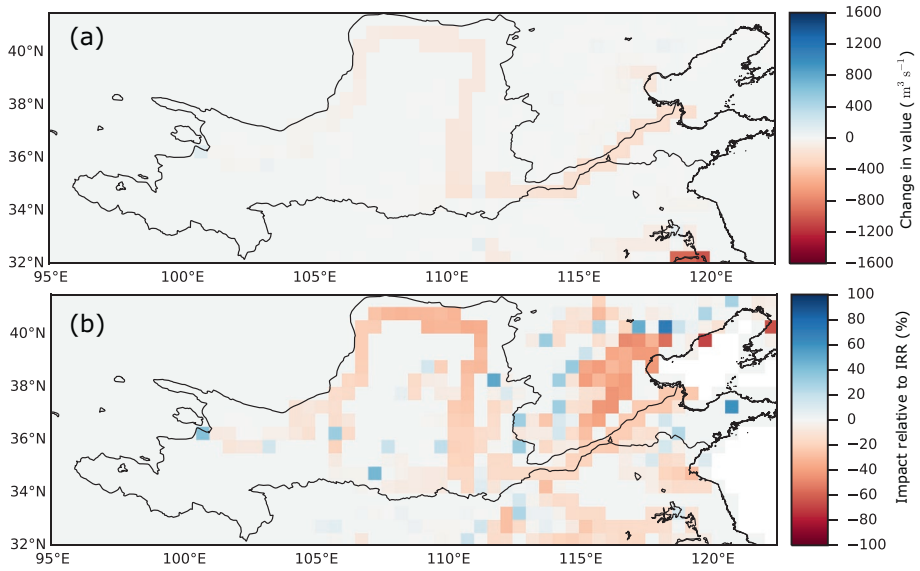

Figure 7. Estimated impact of dams on river discharge relative to the IRR scenario (REG-IRR) (a) in absolute values and (b) as relative change over the 1979–2000 period. IRR, irrigated; REG, regulated.

tributaries is also lower than in the main channel (Figure S5, −24.9% and −22.5% for tributaries and −30.8% for the main channel before confluence). They do not have much effect compared to the one in spring.

This analysis demonstrates that the irrigation impact on the river discharge can vary significantly over time and space because of the complex nature of hydrological topology and the seasonal cycle of river levels. The impact propagates downstream and combines with the changes in tributaries. The impact of irrigation on a river's discharge has to be considered as an accumulated metric over the entire basin. Analysis of the seasonality is also interesting to better reveal the consequences of agricultural abstractions.

4.4. Impact of Dam Regulation on River Discharge

Dams and their regulation rules are mainly designed to increase the water available for human demand by modifying the intra- and inter-annual distribution of the streamflows. Storing water in winter and autumn to be released in spring and summer is especially important for agriculture in the Yellow River basin where water is a limiting factor and not necessarily available from precipitations and glacier melt during the crop growing season. That being said, precipitation is important during summer in the YRB, which is also the crop growing season, which means that reservoirs are not as critical for intra-annual regulation in this region as in other regions. For instance, the Mediterranean region where low precipitations are in summer during the crop growing season. In other catchments in China, in particular the Yangtze River, water is more abundant and both inter and intra-annual regulation on river discharge are less critical.

Figure 7 displays the annual mean difference of discharge between simulations REG and IRR in absolute and relative values. Most grids traversed by the river display a decreased discharge in REG as water available for irrigation and abstraction increases. The cumulative effect of water management increases from the source regions down to the central region of the Yellow River near the Tongguan gauging station. However, as shown in Figure 7, discharge at grids just downstream of a dam often display an increase because the releases in response to demands will only be consumed progressively. As tributaries are generally equipped with smaller dams changes there are less visible.

The seasonality of river discharge, irrigation demands and regulation cycles (Here represented by flood absorption capacity), lead to an impact which also varies significantly throughout the year (Figure 8). The overall impact on the mean annual river levels is relatively small (Figure 7b) but the magnitude of the seasonal changes can be much larger. For instance dams increase the river discharge by over 400% between the

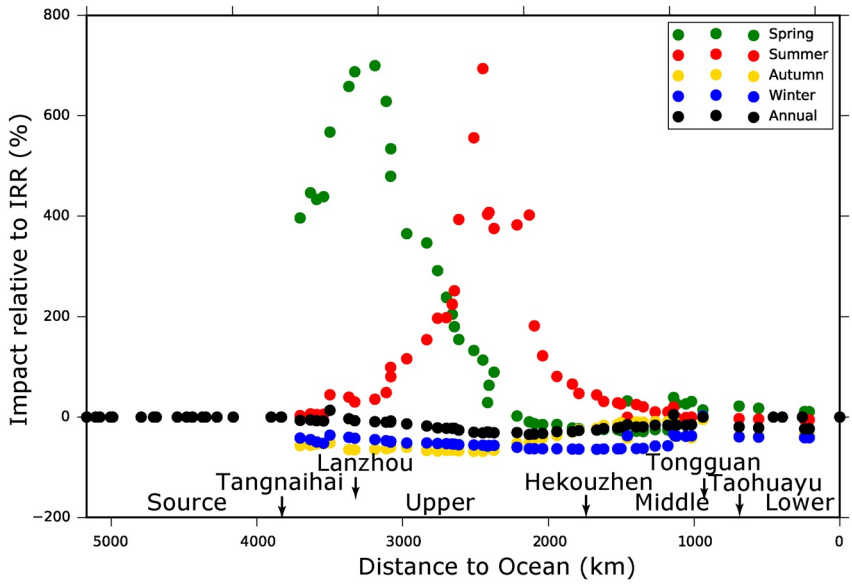

Figure 8. The impact of dam regulation relative to the estimated discharge of the yellow river along its main channel in the IRR scenario (REG-IRR). The long term averages (1979–2000) of annual as well as seasonal flows are displayed. The discrete dots represent the grids along the main river channel. The named stations are positioned on the map in Figure 2. IRR, irrigated; REG, irrigated.

Longyangxia-Liujiaxia cascaded dams and the Tongguan gauging station in spring and summer (Figure 8). Irrigation without dam regulation reduces river discharge to very low levels (Figure 6), but the cascading dams provide large storage which can fulfill unsatisfied irrigation demands downstream through regulation and compensate flow reductions in the irrigation season.

In spring, the positive impact is maximum around the Lanzhou gauging station downstream of the Liujiaxia dam (see Figure 2). The impact decreases progressively as the released water is consumed by abstractions for irrigation (Figure S6a). However, because the additional water released by the dams is used to satisfy a larger fraction of the irrigation demand, consumption increases. Thus, evaporation over the Neimenggu province irrigation districts increase and the river levels are below those of the IRR simulation between the Hekouzhen gauging station and the confluence with the Wei and Fen rivers. The dams on these tributaries meet the irrigation demand in spring and thus bring more water to the main channel than in the IRR simulation leading to a positive impact of regulation down to the outflow point.

In summer, the dams also increase the water available for irrigation and the river discharge (Figure S6b). The positive impact on the river discharge propagates down to the Tongguan gauging station. The changes in summer are not fully attributable to irrigation demands as the dams operate during this season also with a smaller volume to manage flood risks. The impact of dam management benefits mostly the region upstream of the Hekouzhen gauging station. Irrigation perimeters of the Wei and Fen river fully exploit the additional water brought by regulation and thus their contribution to the main channel is reduced leading to smaller differences compared to IRR down to the estuary.

In autumn and winter, the discharge decreases as there is less irrigation demand downstream. Dams do not spill since they have been emptied to satisfy demands and there is no need to leave space for flood attenuation (Section 2.2.2). This allows to fill the reservoirs and prepare for the demands of the following year. The impact is higher in autumn than in the winter (Figures S6c and S6d) because the dam storage period often starts in autumn when the river flow is still high. Consequently, the downstream demands will not be negatively affected by the reduced discharge.

Dam regulation increases the complexity of discharge changes, especially along the main river channel. Reservoir operation can ensure a better demand/supply balance in the different seasons. The water stress

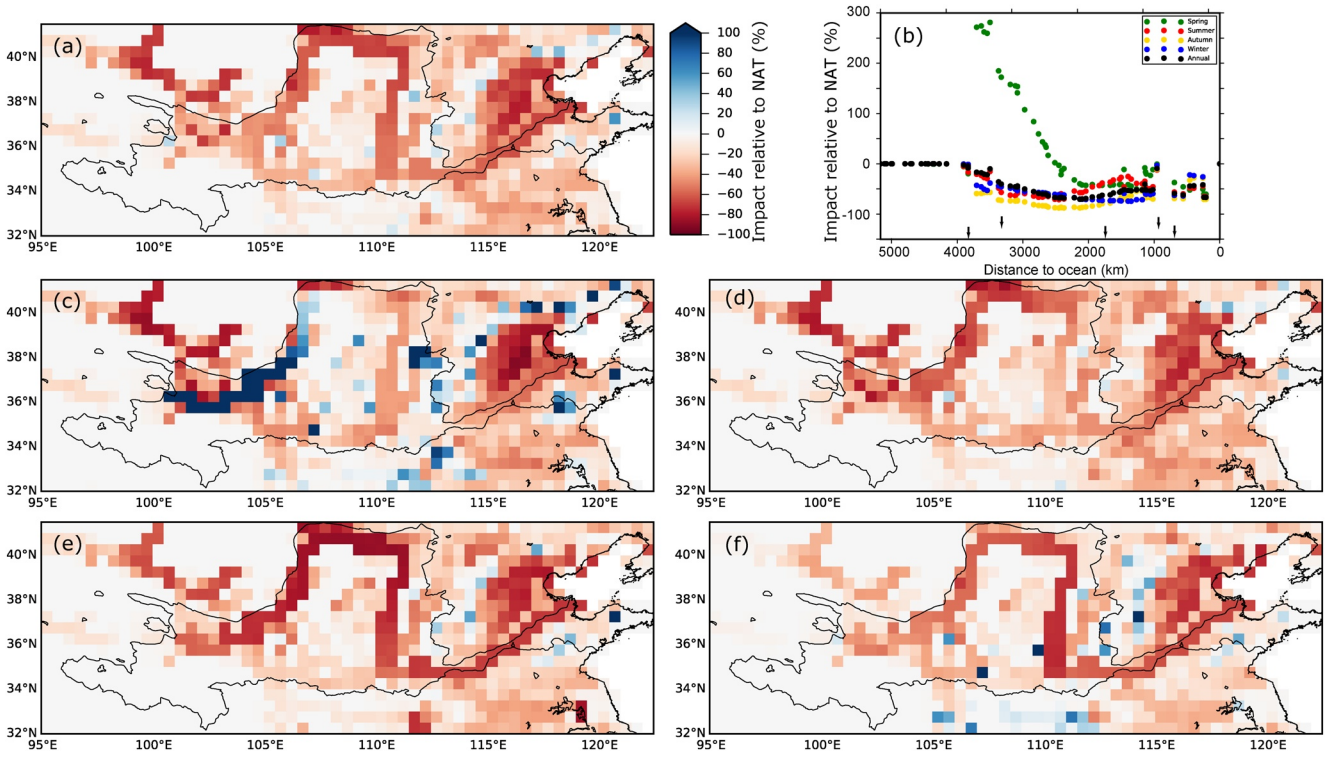

Figure 9. Estimated impact of irrigation and dam regulation (REG-NAT) on river discharge for annual means (a) and the four seasons averaged over the 1979–2000 period: (c) spring, (d) summer, (e) autumn, and (f) winter. The relative change along the main channel is shown in panel (b) using the same layout as Figure 8. IRR, irrigated; NAT, natural.

along the river channel is significantly alleviated because of the regulation in spring and summer, and streamflow is increased. In autumn and winter reservoirs filling leads to a decrease of the flows, though without an increase in water scarcity as irrigation demands are low in these seasons. Extra water abstractions in the upstream catchments could increase the risk of water scarcity downstream if the water demands were not propagated upstream until satisfied.

These interactions between demands and dams releases in an anthropogenized water cycle and their seasonal changes can only be represented when demands and dam regulations over the entire basin are modeled together.

4.5. Overall Impact of Irrigation and Dam Regulation

The overall impact of human water management, that is the combined effects of irrigation and dam regulation, on river discharge is displayed in Figure 9. Because dam regulation increases water availability for agricultural consumption, the annual mean discharge is more strongly reduced in the main channel for the IRR scenario (Figure 7b). In spring, the river discharge turns from decreasing (in IRR) to increasing (in REG) with the additional release from the dams (Figure S6a). The increased river levels last until the main irrigation district of the Neimenggu province. Dam regulation increases river discharge in summer as well, although the discharge is still lower when compared to the natural state. The releases alleviate the water stress especially in the river segments between the Lanzhou and Hekouzhen gauging stations (compare to Figure S6b). Discharge in autumn and winter further decrease when compared to NAT as water is stored in dams for water consumption of the following year. The impact is largest in autumn over the river segment upstream of Hekouzhen gauging station, while in winter the middle reaches of the Yellow river are more affected. Overall, the relative discharge changes are, similarly to the IRR case, within the −50% to −80% range, but they are more homogeneously distributed over the course of the main channel in all seasons except spring due to dam regulation.

Upstream of the Neimenggu province irrigation districts, there is a small dam (Figure 3) but it does not have the capacity of the infrastructures installed more upstream, in particular the Longyangxia-Liujiaxia cascaded dams, and could not by itself support those irrigation districts. In spring, upstream dams release, in the model, large amounts of water (2–3 times the natural discharge) which will not be abstracted for the next 1,500 km. The downstream irrigation districts demand this additional release, in particular the Neimenggu province irrigation districts. Using traditional implementations of dams in hydrological models, dams can only serve regions within a range of 250–1,300 km (see Introduction). Thus, the irrigation districts in Neimenggu province would not benefit from the cascading dams upstream of the Lanzhou gauging station in these settings.

4.6. Impact of Human Water Management on River Discharge at Gauging Stations

The impact of irrigation and dam regulation on river discharge has been investigated over the YRB in the previous sections. Although the irrigation water demand is difficult to evaluate, because of the lack of data, the impact of irrigation water abstraction on the discharge can be used as an indirect test of the irrigation demand estimation. The credibility of the spatial patterns and seasonal changes can also be qualified at gauging station where observations exist. Moreover, with the naturalized river discharge estimated with known management practices, the quality of the simulated impact of human water management can be assessed. Figure 10 displays the comparisons of observed and naturalized discharge with the modeled values in the NAT, IRR, and REG simulations.

Four discharge gauging stations (Tangnaihai, Lanzhou, Hekouzhen, and Lijin) located along the main channel of the Yellow river are used here. Tangnaihai records the river discharge flowing out from the source region where there is very little human intervention. ORCHIDEE underestimates natural discharge especially in spring and summer which is probably caused by the lack of glacier melt and groundwater recharge in the model (Figure 10a1) (Zhou et al., 2018). Due to this limitation, the annual cycle of discharge is displaced to the end of the year in the model, leading to difficulties in filling reservoirs in winter which then impacts dam management. The difference between observed and naturalized discharge established by the basin agencies (black line in Figure 10a3) is very small and comparable to the irrigation abstraction calculated by our model (green line in Figure 10a3).

Discharge of the NAT simulation at the Lanzhou station is also underestimated (blue line in Figures 10b1 and 10b2), with more than 75% of the underestimation being propagated from the source region. Irrigation consumes water and the peak value for the irrigation simulation is in summer (red line in Figure 10b3). On average, the reservoir stores water from August to February when the water level in dam reservoirs is lower than the upper limit, the discharge in the REG simulation is lower than that of the IRR simulation in summer (Figure 10b2). The period when discharge is reduced by human water management (irrigation and dam storage) is longer than the one estimated through the difference between the observed and naturalized discharge.

This can be explained by the underestimated natural discharge simulated by ORCHIDEE. River levels are insufficient to fill the reservoirs over the period from September to the end of December. The downstream demands and the need to lower the dam level in preparation for flooding period force the release of water from February to April which sustains the discharge in spring. If the model would provide a more realistic discharge in the source region of the YRB, the regulated flows would probably be better simulated.

Without regulation, the irrigation demand reduces rivers levels to its minimum in May. Annual evaporated water from anthropogenic water use and management can be estimated by the average difference between actual and naturalized discharge, and is largely attributable to irrigation. In the Tangnaihai-Lanzhou section irrigation water consumption is thus around 90 $m^3 s^{-1}$ (Table 1). In the simulation, irrigation consumption is overestimated in the IRR scenario with 190 $m^3 s^{-1}$. In the REG scenario, water regulation allows to slightly increases consumption to 200 $m^3 s^{-1}$. Although less important than natural discharge underestimation, irrigation demand overestimation contributes to the error of estimated regulated flows.

In the Tangnaihai-Lanzhou section, both irrigation demand satisfaction, reservoir filling and response to downstream demands contribute to modifying river flows. We cannot distinguish the relative magnitude

10.1029/2020WR028133

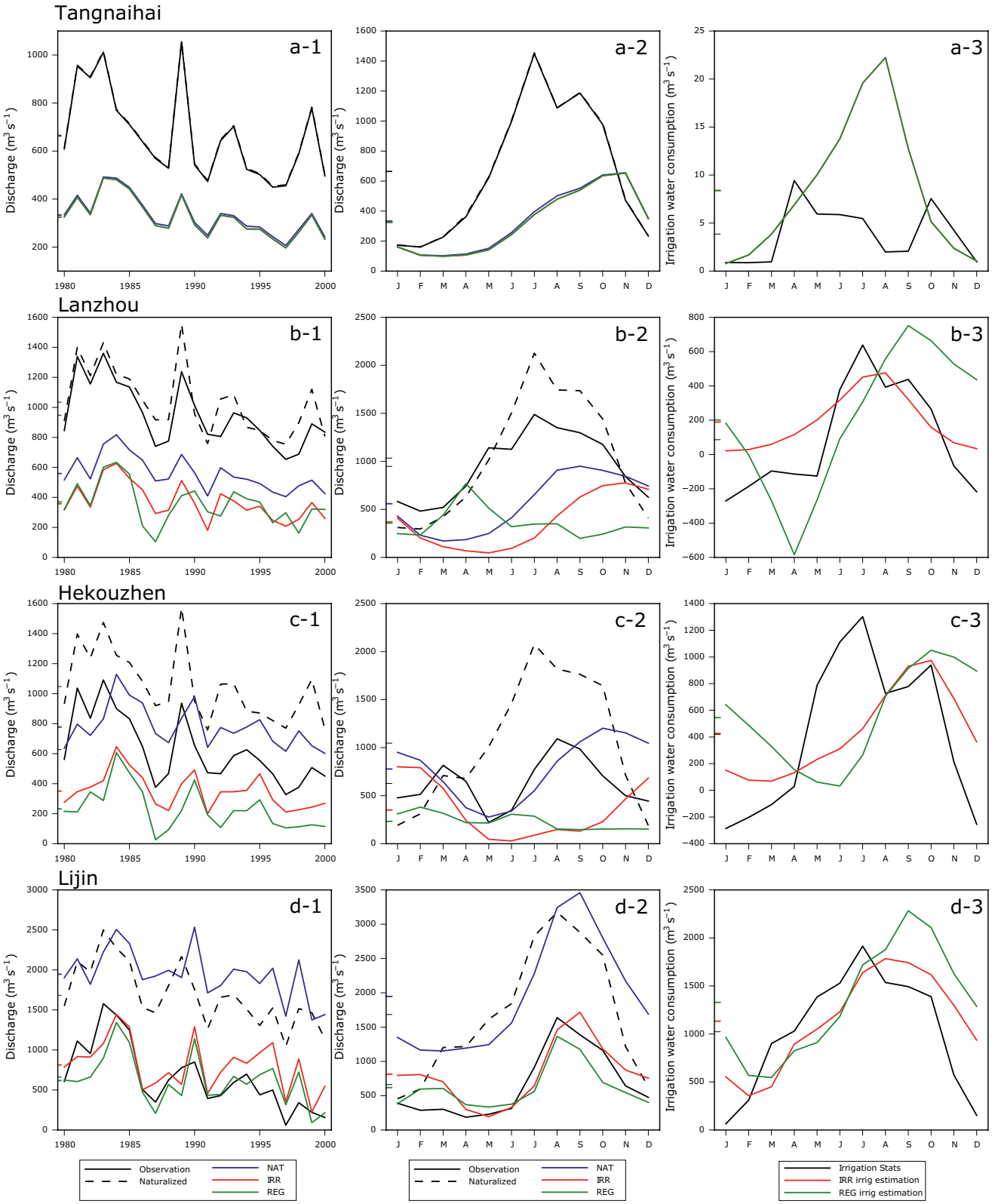

Table 1
Mean Discharge at Different Gauging Stations Along the YRB (unit: $m^3 s^{-1}$) and the Estimated Changes due to Human Water Management

No	Gauge	Observed	Naturalized	Change (%)	NAT	IRR	Change	REG	Change (%)
1	Tangnaihai	662.4	666.2	−0.6	332.6	324.2	−2.5	324.2	−2.5
2	Lanzhou	948.0	1034.5	−8.4	557.0	369.0	−33.7	357.1	−35.9
3	Hekouzhen	627.3	1047.3	−40.1	777.7	352.6	−54.7	233.0	−70.0
4	Lijin	660.6	1683.6	−60.8	1942.5	813.3	−58.1	617.3	−68.2

Note. The reference are the observed and naturalized discharge values provided by the basin agencies. For the model the NAT scenario is compared to the IRR and REG scenario.
IRR, irrigated; NAT, natural; REG, irrigated; Yellow river basin.

of those effects in the difference between the natural inflow into the section and the observed discharge. Therefore, explaining the differences between the REG and the observed inflow is not straightforward. The bias in inflow is very large, however, it will necessarily lead to an underestimation of discharges because reservoirs will not fill nor spill, and reservoirs will often be at a lower operation level than designed for electricity production and storage for future potential water usage. In the REG simulation, dams are operated to lower the water level before the flooding season, which sustains the discharge and satisfies the downstream demands in spring.

At the Hekouzhen gauging station, which is located after the major irrigated areas of the Yellow River basin, the bias in the NAT simulation is also large, with a more pronounced phase shift. The naturalized river discharge at this station increases from January to July, while the observed discharge starts to decrease in April. Given that there is no big dam between Lanzhou and Hekouzhen that could be filled, this indicates the spring time increase in consumptive water use in this river section. The lack of water in upstream dams between May and August as described above results in an underestimation by the model of the water used for irrigation over that period. The shift of maximum natural discharge toward winter on the other hand results in an overestimation of the impact of dam regulation. A large proportion of the inflow will be stored in the dam to compensate for the underestimated inflows since September. The REG simulation maintains higher low flows in the river compared with the IRR run in the summer period, in order to satisfy downstream demands.

The Lijin gauging station is the most downstream and provides an integrated view of the entire YRB. Here, the simulated natural discharge is comparable to the naturalized river discharge provided by the basin agency (blue and dashed black lines in Figures 10d1 and 10d2). The overestimation in other tributaries along the middle and lower river basin compensate the discharge underestimation from the source region of the Yellow River described above. Comparison of the REG and IRR simulations shows that the dam regulation lowers mean discharge and brings it closer to observations (from +23.1% in IRR scenario to −6.6% in REG scenario). It also allows to increase systematically water consumption for irrigation by 24.1% (196 $m^3 s^{-1}$). High flows are advanced by one month which improves the timing of the simulated hydrograph. The discharge reduction simulated for IRR and REG relative to NAT is now comparable to the difference between the observed and naturalized values provided by the basin agencies (Figure 10d3). This shows that over the entire YRB the model has some skills in predicting the current water management in the basin.

Figure 10. Observed, simulated and naturalized discharge for four gauging stations along the Yellow river. From the top to the bottom rows are the results of stations (a) Tangnaihai, (b) Lanzhou, (c) Hekouzhen, and (d) Lijin. The first column (labelled with -1) depicts at each station the annual mean discharge observed, naturalized and for the three simulations (NAT, IRR, and REG). The second column (labelled with -2) provides the mean annual cycle of discharge. The final column (labelled with -3) shows estimates of the effect of management on monthly means by substracting observed from naturalized discharges (black line) and the difference between the simulations IRR and NAT (red line) for the effect of irrigation consumption, as well as REG and NAT (green line) for the overall effect of water management and use. IRR, irrigated; NAT, natural; REG, irrigated.

5. Discussion

5.1. Test Implementation of the New Routing Model

This study proposes a model to represent human water management to be integrated into a LSM and its river routing scheme which are designed for global and regional climate studies. The model represents the adduction network for irrigation, the propagations of water demands and dam regulation methods which balances demands and supplies. This new parametrization of anthropogenic water usage is tested on the Yellow River basin taking advantage of the existence of observed and naturalized discharges provided by the basin agency. The implementation shows the qualities of the newly incorporated modules especially at the Lijin gauging station (Figure 10d) where the simulated discharge for the managed river and the theoretical natural system is consistent with the values observed and naturalized by the basin agencies. Large errors and uncertainties remain at other gauging stations with a smaller upstream area (Figures 10a–10c), indicating that multiple error sources compensate in the lower sections of the YRB. This shows that evaluating mode over large basins only, Mississippi (Hanasaki et al., 2006), or Colorado (Haddeland et al., 2006), for example, is not very adequate since errors over smaller regions can compensate. This study also highlights that the natural flows, which are mainly driven by the climate, are still a challenge to simulate. Despite these uncertainties, the discharge alteration due to human activities as implemented in the proposed model are in relatively good agreement with the impact of water management practices as they can be derived from the naturalized flows provided by basin agencies. Irrigation mainly decreases river discharge, while dam regulation allows to increase water availability for agricultural abstractions, further reducing the river levels as a result. The seasonal changes also demonstrate the role of dams in changing the annual cycle of river discharge. A better representation of natural discharge would be needed to check more precisely to what extent representing anthropogenic management improves the accuracy of the modeling. Even if natural discharges were represented more adequately, more detailed data on reservoir volumes, irrigation abstraction and consumption, at a monthly time step, for instance, would be needed to fully check the different elements of the modeling. Otherwise errors could still compensate on sections where both irrigation and reservoir operation are present.

In addition to the investigation on the river discharge at gauging stations, this study indicates that the proposed integration of the irrigation demands into the hydrological graph is important. The estimated demand/supply path density, which takes into account the existing river network and topography, corresponds well to the known irrigated perimeters and the distribution of water. Transfer distances are broadly consistent with existing infrastructures, although some spurious long-range associations persist. The approach proposed here is superior to the simple assumption that within a certain radius around the demand point a water source can be found. The simulated human impact from the upstream to downstream along the main channel helps to understand its propagation and interaction with local demands. The steep changes after dams or at confluences of large rivers demonstrate the ability of the model to capture the operation of the dams in relation to its location in the hydrological network and in balance with major regions of agricultural demands.

In this study, we chose the Yellow River Basin as our first test region mainly because the naturalized river discharge is available from local basin management agencies at several gauging stations along the Yellow River. With naturalized river discharge, we can evaluate how the model performs under natural conditions (without human interventions). Additionally, the Yellow River is a continental-level river which spans different climate zones. It contains a large proportion of China's population and agricultural areas and faces today water scarcity in different subregions. The relatively simple river channel and the distribution of dams (mainly on the mainstream) is helpful to attribute the biases noted in the simulation. In the next steps, this model will be adopted to other climates in different climatic zones and with different intensity of human water management.

5.2. The Original Contribution of the Proposed Approach

Despite the intrinsic difficulty to evaluate a model of water management practices for a given region, the design of the proposed scheme offers an original approach which allows to eliminate some hypothesis used in other models and in particular those which assume a known stationary climate (Milly et al., 2008).

1. The main climate dependant water demand, irrigation, is explicitly simulated by the LSM
2. The unsatisfied water demand in a given region can propagate upstream. This enables all dams within a catchment to operate as a system. In previous approaches, dams only respond to demands within a certain user-defined distance
3. Very few assumptions are made on the dams' operating rules. As the demand propagation and dam regulation operate at sub-diurnal time steps (no shorter than the routing integration step: 1 h) the system can respond to rapid changes in demand and supply or flooding events driven by climate. The model is thus suited to analyze the feedbacks between climate variability and change and the human water management and use
4. The water management scheme is designed on the basis of the HTU concept used in ORCHIDEE and thus can take into account the complexity of the hydrological network which would be lost on a typical atmospheric grid. This allows to resolve important heterogeneities within the large-scale grid and helps to accurately locate infrastructures for water management. High-resolution routing units also ensure accurate hydrological connectivity between the location of the demands and the regulation points
5. The implementation of a simple maximization model connects the demand points to the potential sources of water. The resulting adduction network has realistic properties, respects topography and is independent of the grid imposed on the LSM by the atmospheric information
6. Using a supply/demand approach to dam regulation gives the model some tolerance to systematic biases in the simulated natural water cycle

5.3. Sources of Uncertainty

The uncertainties in the simulated discharge result from three main sources: the climate forcing and the representation of the natural hydrological processes, the estimation of the irrigation demands and the modeling of human water management. Uncertainties in the forcing variables and in the land surface model's structure and parameters will propagate to the runoff and drainage estimations (Bhuiyan et al., 2019; Zhou et al., 2018) thus providing a skewed basis for simulating water management. Furthermore, they affect the estimation of climate-related water demands. In the test over the YRB presented here, the lack of a proper representation of glaciers and groundwater in ORCHIDEE is the most likely limitation in addition to the uncertainties in the climate forcing. This underestimation of the inflows propagates downstream, in the filling period as missing spills and in the irrigation season as unsatisfied demands, increasing the difficulty to analyze the performance of the water management model as it biases the supply side.

Different methods have been tested to estimate irrigation water potential demands. Either the irrigation water aims to satisfy the transpiration demands of crops (Guimberteau, Laval, et al., 2012) or to alleviate the soil moisture deficit in the grid box (Yin et al., 2020). Irrigation techniques also affect the water demand and vary with regions and with crops leading to different efficiencies and return flows. Drip irrigation is more widespread in semi-arid regions while flood irrigation is more often used in southern China especially for rice paddy. Uncertainties in the water needs for irrigation will also affect the assessment of the model and bias the simulation of the demand side. Thus, the model's sensitivity to the irrigation representation should be considered in future studies.

5.4. The Water Management

The third source of uncertainty is associated with the representation of the human water management. In this implementation over the YRB, not all aspects of human water management could be considered. For instance, water demand from the domestic and industrial sectors are not yet included. But since these two water usages are mostly non-consumptive (Shaffer & Runkle, 2007), large parts of the abstracted water will return to the rivers downstream (Neverre et al., 2016). Since these demands are smaller than the irrigation demand, their impact on the river levels is expected to be small on most time scales.

In the current implementation, fossil groundwater withdrawals are not considered. The availability of fossil groundwater is unknown and its usage is restricted by local government. Although fossil groundwater withdrawal has been included in some models (e.g., H08 Hanasaki et al., 2010, WaterGAP Müller Schmied

et al., 2021, and PCR-GLOBWB Sutanudjaja et al., 2018), they assume unlimited fossil groundwater which can be pumped without constrains or as a proportion of surface water. Such a solution is not feasible in an Earth System Model, more specifically in its land surface component, as it creates an open boundary in the water cycle. Neglecting fossil groundwater here leads to some uncertainties on the satisfaction of water demands, but should not affect significantly our results on the simulated river discharge.

The ecological or environmental flow which represents the lowest limit of permitted river discharge is only partially accounted for here as the definition has still to be clarified (Poff & Zimmerman, 2010; Poff et al., 2010). On the other hand, defining thresholds for ecological flows is difficult, and even more when the statistics of the simulated natural flows are biased. In this study, the ecological flow is not considered as a constraint for water management. Dam regulation, even if based only on irrigation demands already raises low flows in spring, but decrease river levels in winter. Adding a constraint on environmental flows would increase the impact of water management on the minimal river levels. The very significant increase of spring discharge can be caused by the underestimation of river discharge under natural condition and the excessive abstraction for other water usages when no threshold is set for the ecological flow.

The rules regulating dams operations have been modeled based on demand satisfactions and flood control. This ensures that reservoirs remain as full as possible, depending on the inflows and satisfy demands as much as possible. In this setting, climate change will impact both sides of the equation, climate-dependent demands, and inflows. The operation of dams will adapt naturally to the changes by finding a new supply/demand equilibrium. In the YRB, for most dams the rules used in current operations are not known, thus direct validation is difficult. Nevertheless, with the general rules proposed here, the model reproduces relatively well the general characteristics of observed discharge, indicating that for the current climate the approach is appropriate. All dams in the YRB can be operated in coordination for flood protection and the coordination is necessary to balance the water supply to different administrative regions along the main river. This is an aspect which is taken into account in our approach but difficult to validate without detailed knowledge of the procedures practised by the basin agencies of the region.

6. Perspective

The proposed scheme for introducing human water management in LSM and thus climate models is based on the need for these systems to reproduce the actual continental water cycle. The supply of water in all catchments is driven by climate. The dominant demands for surface water, agriculture, is strongly modulated by climate as well. As these processes are already represented in LSMs, it is natural to view the human intervention in the water cycle as an effort to better balance supply and demand at catchment scales and throughout the annual cycle.

The model presented here attempts to implement this vision while trying to use as few hypotheses as possible on the current rules used to manage water resources. It requires to introduce in our model value classes for water allocation based on the social and economical importance of the different demands. We believe that the four broad classes we have chosen are sufficient for climate applications. The model also tries to integrate the constraints imposed by the hydrological network as precisely as possible as these are time-invariant properties fundamental to the horizontal fluxes in the continental water cycle.

In addition to improving the representation of the water cycle, estimating the water actually available for irrigated crops could improve the carbon cycle representation in LSM. Representing human water management more realistically also opens the possibility to assess the consequences of adaptation measures or changes in management.

We have performed a first evaluation of this approach over the highly managed Yellow River basin but with a number of simplifications. Other demands than irrigation have not yet been considered. This simple implementation already reveals that biases in the simulated natural flows are currently a strong limitation. Lack of information on actual dam management and on the water allocations for irrigation and the actual consumption also limits the validation of such a model. Other more data-rich areas will have to be explored in order to pursue the validation of the model. Over the YRB only the mean annual cycle was analyzed be-

cause of the relatively short period of available data, especially the naturalized river discharge from water agencies. Longer time series, which might be available in other regions, will permit to test the ability of the model to simulate the impact of human water management on the variability and trends in river discharge. The model will also need to be enhanced with the representation of hydro-power and domestic water usage as these are major water using sectors, in value if not in quantity.

We have presented the strategy proposed for the ORCHIDEE LSM but other approaches are certainly possible. The major constraints for any such developments are that parametrizations of human water management should not assume that the climate drivers are stationary and the full information on the continental water cycle available in LSMs should be used. The various representations of human water management which are being developed by the community will be essential tools to attribute past changes in water resources to evolutions of land and water use as well as climate variability and change. These developments are essential for climate and hydrological sciences as they will build our confidence in the projected water resources for a future climate.

Appendix A: Indexing convention of the adjacency matrices

The relations between the vertices of the river graph are represented by an index. The natural flow direction of the river is used to order the indices of the water stores on the graph. We note $\{i-1\}$ the ensemble of all stores upstream of vertex i and $i+1$ the one downstream. The flux of water between stores are placed on the edges of the graph and are indexed with half indices. Because the graph is a tree, each vertex is linked to an ensemble of upstream vertices but only one downstream, thus for the edges we have $i+1/2 \in \{(i+1)-1/2\}$. The water flowing into the stores of i is given by the ensembles of fluxes on edges $\{i-1/2\}$ while the outflow is given on the edge $i+1/2$.

The same indexing applies to demands near the river bed which are generated directly on the vertices and transmitted on the edges. The ensemble of vertices l using water from i for irrigation through the adduction edges are labeled $\{l\}i$. This allows to index the water fluxes and demands simulated between the water adduction point in the river vertex and irrigated vertices. As the ensemble $\{l\}i$ are leaves of the tree, the fluxes are not placed on half indices.

Each HTU (vertex) i is associated to grid box $\hat{i}$ which can be different or the same as $\widehat{i+1}$. The grid cell associated with each HTU is needed for the source and sink terms of the routing scheme which are computed by ORCHIDEE on the grid of the atmospheric forcing data. We define $\delta_{i,\hat{i}}$ as the fraction of the mesh $\hat{i}$ occupied by the HTU i.

Flood plains areas are not added in current ORCHIDEE (Schrapffer et al., 2020). Floodplain areas can have divergent flows, in which case, the vertex has more than one outflow path. The multiple outflows from a given vertex do not create cycles in the graph because we are in a digraph (Foulds, 1992), that is, the water cannot flow back. The water diverted for floodplains or irrigation is governed by different processes and will travel through the ORCHIDEE soil moisture before coming back into the routing network.

Appendix B: Water Continuity Equations

B1. Prognostics equations for the stream store

The over-land flow, the most accessible water, is governed by the following prognostic equations:

$$k=0: \frac{dW_{stream,i,k}}{dt} = \left(\{Fs_{i-\frac{1}{2},k}\} - Fs_{i+\frac{1}{2},k}\right) + \frac{W_{fast,i-1}}{g_2\tau_{i-1}} + \frac{W_{slow,i-1}}{g_3\tau_{i-1}}, \quad \text{(B1)}$$

$$k = 1: \frac{dW_{stream,i,k}}{dt} = \left(\{Fs_{i-\frac{1}{2},k}\} - Fs_{i+\frac{1}{2},k} \right) + \frac{W_{fast,i-1}}{g_2 \tau_{i-1}} + \frac{W_{slow,i-1}}{g_3 \tau_{i-1}} + \tag{B2}$$

$$-e_{i,1} - \sum_{k=2\ldots4} e^1_{i,k} + r_{i,2} + r_{i,4}, \tag{B3}$$

$$k = 2\ldots4: \frac{dW_{stream,i,k}}{dt} = \left(\{Fs_{i-\frac{1}{2},k}\} Fs_{i+\frac{1}{2},k} \right) - e_{i,k}. \tag{B4}$$

$Fs_{i+\frac{1}{2},k}$ is the river flow along the edge $i + 1/2$ for class k. The volume of the stream store is regulated by the difference between the sum of inflows ($\{Fs_{i-\frac{1}{2},k}\}$ an implicit summation is meant here) and outflow ($Fs_{i+\frac{1}{2},k}$) and, in the case of non-reserved surface waters ($k = 0$ and $k = 1$), the contribution of the two aquifers. The regulated part of the stream ($k = 2$, ...4) includes also the three types of local extractions ($e_{i,k=2,3,4}$) and does not benefit from the inflow of stores as they only contribute to ecological fluxes. g_1, g_2, and g_3 are the time constant for three different stores respectively. In this study, they are specific as 0.05, 0.3, and 7.0 in unit (day km^{-1}). τ_{i-1} is the topographic index which is calculated for each HTU.

For the ecological and non-reserved flow reservoir ($k = 1$) another contribution is the non-consumptive water usages (hydro-power, industrial, and domestic usage) which return to the stream within the same HTU ($r_{i,2} = e_{i,2}$, $r_{i,4} = e_{i,4}$). There is no need for an explicit return flow for irrigation as the corresponding abstractions are added to soil moisture and thus rejoin the natural water cycle or ORCHIDEE. In case a demand cannot be satisfied with its reserved water and there is no stress on the ecological reservation, water can be extracted from the ecological flow. This transfer of demands onto the non-reserved flow is labeled: $e^1_{i,k=2,3,4}$. This set of equations describes a system were at the sources of the rivers all the water is considered to be ecological non-reserved flow and it is only progressively, through regulation at dams, that water is brought to the other stream stores.

The flux out from stream store of HTU i and class k is given by:

$$Fs_{i+\frac{1}{2},k} = \frac{W_{stream,i,k}}{g_1 \tau_i}. \tag{B5}$$

This formulation ensures that the sum of all classes brings the model back to the previous formulation of the model as $g_1 \tau_i$ is independent of the value class.

For a segment without abstractions (natural condition), the model produces the following relations:

$$Fs_{i+\frac{1}{2},0} = \sum_{k=1}^{k=4} Fs_{i+\frac{1}{2},k} \text{ and} \tag{B6}$$

$$W_{stream,i,0} = \sum_{k=1}^{k=4} W_{stream,i,k}. \tag{B7}$$

The fast aquifer represents a storage with a short residence time. It is the recipient of the surface runoff ($R_{\hat{i}}$) generated by the soil moisture scheme of ORCHIDEE

$$\frac{dW_{fast,i}}{dt} = -\frac{W_{fast,i}}{g_2 \tau_i} + \delta_{i,\hat{i}} R_{\hat{i}}, \tag{B8}$$

$\delta_{i,\hat{i}}$ as the fraction of the mesh $\hat{i}$ occupied by the HTU i.

The slow aquifer represents a storage with long residence times. It receives the deep drainage of the soil moisture model ($D_{\hat{i}}$).

$$\frac{dW_{slow,i}}{dt} = -\frac{W_{slow,i}}{g_3\tau_i} + \delta_{i,\hat{i}} D_{\hat{i}} \,, \tag{B9}$$

where $D_{\hat{i}}$ is the deep drainage of the grid box in which HTU i is located.

B2. Water bodies

Lakes or reservoirs can cover large areas and thus be distributed over a number of HTUs or vertices in the graph. It is thus necessary to include the formation and expansion of the water bodies within the graph.

For each water body, the maximum storage capacity is known ($Vref_i$). This information is important as it will determine where these water bodies can form and needs to be simulated. The GLWD database (Lehner & Döll, 2004) provides the volume and a polygon to define the water body. This information is used to identify which vertices in the graph are part of the lake/reservoir ($Vref_i > 0$) and divide the volume over these vertices according to their area. Elsewhere the surface storage volume ($Svol_i$) is zero. We can thus calculate the storage capacity and the current storage of the water body flowing out at i as:

If $Svol_i > 0$ and $Svol_{i+1} = 0$:

$$Vref_i = \sum_{j=i}^{\text{while } Svol_j > 0} Svol_j \,, \tag{B10}$$

$$V_i = \sum_{j=i}^{\text{while } Svol_j > 0} \sum_{k=1}^{4} W_{stream,j,k} \,. \tag{B11}$$

Else:

$$\begin{aligned} Vref_i &= 0 \,, \\ V_i &= 0 \,. \end{aligned}$$

The vertices which contain the dam or the sill which controls the water body are characterized by $Svol_{i+1} = 0$ and $Svol_i > 0$. If $Svol_{i+1} > 0$ and $Svol_i > 0$ then both vertices are part of the same lake/reservoir.

To parametrize the release function of dams the volume of the reservoir at the outflow point and the sum of all upstream volumes are needed. Thus the upstream stored volume Vu_i and capacity $Vuref_i$ need to be computed. They are determined iteratively along the graph from the leaves to the root:

$$Vu_0 = 0 \quad \text{and} \quad Vuref_0 = 0 \,, \tag{B12}$$

$$Vu_i = \sum_{j \in \{i-1\}} V_j \,, \tag{B13}$$

$$Vuref_i = \sum_{j \in \{i-1\}} Vref_j \,. \tag{B14}$$

In order to ensure that the stored water is equally distributed over the vertices which make up the water body, stream flow equations are modified for the three following cases: A river flowing into the water body, exchanges within the lake and outflow from the lake.

$$Svol_i = 0 \text{ and } Svol_{i+1} > 0: \quad Fs_{i+\frac{1}{2},k} = \frac{W_{stream,i,k}}{g_1\tau_i} \,, \tag{B15}$$

$$Svol_i > 0 \text{ and } Svol_{i+1} > 0: \quad Fs_{i+\frac{1}{2},k} = \frac{W_{stream,i,k} - W_{stream,i+1,k}}{2}, \tag{B16}$$

$$Svol_i > 0 \text{ and } Svol_{i+1} = 0: \quad Fs_{i+\frac{1}{2},k} = Re_{i+\frac{1}{2},k}, \tag{B17}$$

where $Re_{i,k}$ is the release flux from the water body.

B3. Floodplains

The above description does not include the floodplains and swamps currently parametrized in ORCHIDEE (d'Orgeval et al., 2008) as they are local to the cell of the atmospheric grid and thus simply diffuse water among the vertices within that cell. In this new interpretation of the model's routing scheme, we will need to reformulate the floodplain parametrization so that it can generate flows from one HTU to more than just one other HTU. Thus the graph will include more than one edge downstream of vertices within the floodplains to generate divergent flows. This is work in progress.

Appendix C: Local Demands and their Fulfillment

C1. Ecological and unallocated flow

The ecological demand is defined as the water needed to avoid water levels in the river below the multi-annual minimal value. This allows to define a demand which will ensure that the upstream dams will release sufficient water to eventually return to the target level. Since there is no anticipation of the low flows, the time to return to the target level depends on the water velocity between the dam releasing water and the demand.

$$dl_{i,1} = \max\left(\min\left(\overline{W_{stream,i,0}}\right) - \sum_{k=1}^{4} W_{stream,i,k}, 0\right). \tag{C1}$$

$\overline{W_{stream,i,0}}$ is the climatology of the natural stream reservoir levels. $dl_{i,1}$ is the total local demand at HTU i for the ecological flow.

The ecological demand in the river is not water which needs to be extracted from the stream but it ensures that dams release water to restore minimal flows in the river. It thus needs to be propagated upstream so that it can contribute information to the dam management. This yields the following equations:

$$du_{i,1} = dl_{i,1} \text{ and } e_{i,1} = 0. \tag{C2}$$

$du_{i,1}$ is the unsatisfied demand and $e_{i,1}$ is water extracted for the ecological flow. Indeed, the ecological flow is still in the river change, here it is a conversion of the water class rather than transferring water to other HTUs.

C2. Domestic and industrial use

Compared to the variability of river discharge or irrigation demands, the domestic and industrial water use is generally constant in time. Moreover, because the domestic and industrial water use is not consumptive, a large portion of the water returns to the system (i.e. $r_{i,2} = e_{i,2}$) (Shaffer & Runkle, 2007). As we neglect it for the moment the following simple equations are used:

$$du_{i,2} = dl_{i,2} = e_{i,2} = 0. \tag{C3}$$

To ensure that water can be abstracted before it has arrived from the reservoir, some specific reservoir could be introduced that will generate a demand when below a given level. Existing water adduction networks have reservoirs which serve as buffers. By introducing them the system can anticipate dam releases or generate earlier demands.

C3. Irrigation

ORCHIDEE simulates a grid box average irrigation demand for crops as formulated in Guimberteau, Laval, et al. (2012). As it is based on the moisture stress experienced by the transpiration of plants, it is controlled by soil moisture and thus changes very progressively. Using the adduction network, the demands of vertices $l\,(\delta_{l,\hat{l}} I_{\hat{l}})$ is added to their corresponding vertex i in the routing graph and thus define an ensemble $dl_{\{l\}i,3}$ positioned on the leaves and have to be satisfied at i.

The irrigation can be extracted from the stream reservoir dedicated to this value class but also from the ecological flow, if there are no unsatisfied ecological demands downstream. Thus the unsatisfied demand for irrigation is:

$$\text{if } d_{i,1} > 0 \text{ then} \qquad du_{i,3} = \max\left(\sum_{\{l\}i} dl_{\,l-\frac{1}{2},3} - W_{stream,i,3}, 0\right), \tag{C4}$$

$$\text{else} \qquad du_{i,3} = \max\left(\sum_{\{l\}i} dl_{\,l-\frac{1}{2},3} - \left(W_{stream,i,1} - \sum_{\kappa=1}^{31} e^1_{i,\kappa} + W_{stream,i,3}\right), 0\right). \tag{C5}$$

$\sum_{\kappa=1}^{3-1} e^1_{i,\kappa}$ is the water amount that has been kept from the stream store for the ecological flow. The rest of the water storage in the stream store can be transferred for irrigation water usage in this case.

The corresponding extractions from the ecological and irrigation value classes are obtained:

$$\text{if } d_{i,1} > 0 \text{ then} \qquad e^1_{i,3} = 0 \text{ and } e_{i,3} = \sum_{\{l-\frac{1}{2}\}i} dl_{l,3} - du_{i,3}\,, \tag{C6}$$

$$\text{else} \qquad e_{i,3} = \min\left(\sum_{\{l-\frac{1}{2}\}i} dl_{l,3} - du_{i,3}, W_{stream,i,3}\right), \tag{C7}$$

$$e^1_{i,3} = \min\left(\sum_{\left\{l-\frac{1}{2}\right\}i} dl_{l,3} - e_{i,3}, W_{stream,i,1} - \sum_{\kappa=1}^{3-1} e^1_{i,\kappa}\right). \tag{C8}$$

The extraction is first performed on the irrigation class reservation ($e_{i,3}$) and then on the ecological flow ($e^1_{i,3}$) if needed, with abstractions for classes with higher priorities served first. When river levels are low, the irrigation demand could be partially unsatisfied until water has come down from the reservoirs. However, soil moisture acts as a buffer such that evaporation can partially be sustained even if the streams are low.

Having the irrigation demand of vertices l which are linked to i through the adduction network $l-\frac{1}{2}$, the extraction in the irrigation class can be distributed proportionally to compute the actual irrigation flux reaching the soil moisture of the corresponding grid box ($Ir_{\hat{l}}$):

$$Ir_{\hat{l}} = \sum_{m=\{l-\frac{1}{2}\}i\in\hat{l}} \frac{dl_{m,3}}{\sum_{\{l-\frac{1}{2}\}i} dl_{l,3}} \left(e_{i,3} + e^{1}_{i,3}\right). \quad \text{(C9)}$$

Two additional processes can easily be introduced into the irrigation demand formulation. Transport losses along the adduction network can be taken into account by augmenting the demand applied to the river network ($dl_{l,3}$) with an appropriate factor. This will increase abstractions relative to the needs of the plants and lead to more return flows. Extraction of the renewable groundwater represented in ORCHIDEE could also be added. Pumping is almost always more expensive than horizontal transfers, thus it could be used as a last resort.

The above equations define a potential or a total irrigation demand which is independent of decisions by farmers or society. These potential demands might not be realized at the extraction point because of an agricultural practice or existing rules. These aspects are outside of the scope of the model.

Data Availability Statement

The present study uses data from previously published sources or data which are distributed by the public organizations which have commissioned them: The codes and explanation for its usage can be accessed from https://gitlab.in2p3.fr/ipsl/lmd/intro/humanwatermanagement. Atmospheric forcing WFDEI-CMA: Zhou et al. (2018). Areas equipped for irrigation: Siebert et al. (2013). ESA land cover map: Lamarche et al. (2017).

Acknowledgments
This study was supported by the National Natural Science Foundation of China (grant no. 41561134016); the CHINA-TREND-STREAM French national project (ANR grant no. ANR-15-CE01-00L1-0L); and the China Scholarship Council (CSC, 201506710042). The work was supported by computing resource of the IPSL ClimServ cluster at École Polytechnique, France. The authors gratefully acknowledge Prof. Feng Zhou for sharing river flow data over the Yellow river basin.

References

Adam, J. C., Haddeland, I., Su, F., & Lettenmaier, D. P. (2007). Simulation of reservoir influences on annual and seasonal streamflow changes for the Lena, Yenisei, and Ob' rivers. *Journal of Geophysical Research*, *112*(D24). https://doi.org/10.1029/2007jd008525

Bhuiyan, M. A. E., Nikolopoulos, E. I., Anagnostou, E. N., Polcher, J., Albergel, C., Dutra, E., et al. (2019). Assessment of precipitation error propagation in multi-model global water resource reanalysis. *Hydrology and Earth System Sciences*, *23*(4), 1973–1994. https://doi.org/10.5194/hess-23-1973-2019

Biemans, H., Haddeland, I., Kabat, P., Ludwig, F., Hutjes, R. W. A., Heinke, J., et al. (2011). Impact of reservoirs on river discharge and irrigation water supply during the 20th century: Impact of reservoirs on discharge and irrigation. *Water Resources Research*, *47*(3). https://doi.org/10.1029/2009wr008929

Cai, X., & Rosegrant, M. W. (2004). Optional water development strategies for the Yellow river basin: Balancing agricultural and ecological water demands. *Water Resources Research*, *40*(8), 1–11. https://doi.org/10.1029/2003WR002488

Chaney, N. W., Metcalfe, P., & Wood, E. F. (2016). Hydroblocks: A field-scale resolving land surface model for application over continental extents. *Hydrological Processes*, *30*(20), 3543–3559. https://doi.org/10.1002/hyp.10891

de Rosnay, P., Polcher, J., Laval, K., & Sabre, M. (2003). Integrated parameterization of irrigation in the land surface model ORCHIDEE. Validation over Indian Peninsula. *Geophysical Research Letters*, *30*(19), 1986–1990. https://doi.org/10.1029/2003gl018024

Döll, P., Fiedler, K., & Zhang, J. (2009). Global-scale analysis of river flow alterations due to water withdrawals and reservoirs. *Hydrology and Earth System Sciences Discussions*, *6*(4), 4773–4812. https://doi.org/10.5194/hessd-6-4773-2009

Döll, P., & Siebert, S. (2002). Global modeling of irrigation water requirements. *Water Resources Research*, *38*(4), 1–10. https://doi.org/10.1029/2001wr000355

d'Orgeval, T., Polcher, J., & de Rosnay, P. (2008). Sensitivity of the west African hydrological cycle in ORCHIDEE to infiltration processes. *Hydrology and Earth System Sciences*, *12*(6), 1387–1401. https://doi.org/10.5194/hess-12-1387-2008

Draper, A. J., & Lund, J. R. (2004). Optimal hedging and carryover storage value. *Journal of Water Resources Planning and Management*, *130*(1), 83–87. https://doi.org/10.1061/(asce)0733-9496(2004)130:1(83)

Ducoudré, N. I., Laval, K., & Perrier, A. (1993). SECHIBA, a new set of parameterizations of the hydrologic exchanges at the land-atmosphere interface within the LMD atmospheric general circulation model. *Journal of Climate*, *6*(2), 248–273. https://doi.org/10.1175/1520-0442(1993)006⟨0248:SANSOP⟩2.0.CO;2

Farrell, P. E., Piggott, M. D., Pain, C. C., Gorman, G. J., & Wilson, C. R. (2009). Conservative interpolation between unstructured meshes via supermesh construction. *Computer Methods in Applied Mechanics and Engineering*, *198*, 2632–2642. https://doi.org/10.1016/j.cma.2009.03.004

Flato, G., Marotzke, J., Abiodun, B., Braconnot, P., Chou, S. C., Collins, W., et al. (2014). *Evaluation of climate models*. In Climate change 2013: The physical science basis. Contribution of working group I to the fifth assessment report of the intergovernmental panel on climate change (pp. 741–866). Cambridge University Press. https://doi.org/10.1017/CBO9781107415324.020

Foulds, L. R. (1992). *Graph theory applications*. New York, NY: Springer. https://doi.org/10.1007/978-1-4612-0933-1

Guimberteau, M., Drapeau, G., Ronchail, J., Sultan, B., Polcher, J., Martinez, J.-M., et al. (2012). Discharge simulation in the sub-basins of the Amazon using ORCHIDEE forced by new datasets. *Hydrology and Earth System Sciences*, *16*(3), 911–935. https://doi.org/10.5194/hess-16-911-2012

Guimberteau, M., Laval, K., Perrier, A., & Polcher, J. (2012). Global effect of irrigation and its impact on the onset of the Indian summer monsoon. *Climate Dynamics*, *39*(6), 1329–1348. https://doi.org/10.1007/s00382-011-1252-5

Haddeland, I., Skaugen, T., & Lettenmaier, D. P. (2006). Anthropogenic impacts on continental surface water fluxes. *Geophysical Research Letters*, *33*(8). https://doi.org/10.1029/2006gl026047

Hanasaki, N., Inuzuka, T., Kanae, S., & Oki, T. (2010). An estimation of global virtual water flow and sources of water withdrawal for major crops and livestock products using a global hydrological model. *Journal of Hydrology*, *384*(3–4), 232–244. https://doi.org/10.1016/j.jhydrol.2009.09.028

Hanasaki, N., Kanae, S., & Oki, T. (2006). A reservoir operation scheme for global river routing models. *Journal of Hydrology*, *327*(1–2), 22–41. https://doi.org/10.1016/j.jhydrol.2005.11.011

Hanasaki, N., Kanae, S., Oki, T., Masuda, K., Motoya, K., Shirakawa, N., et al. (2008). An integrated model for the assessment of global water resources—Part 1: Model description and input meteorological forcing. *Hydrology and Earth System Sciences*, *12*(4), 1007–1025. https://doi.org/10.5194/hess-12-1007-2008

Hanasaki, N., Yoshikawa, S., Pokhrel, Y., & Kanae, S. (2018). A global hydrological simulation to specify the sources of water used by humans. *Hydrology and Earth System Sciences*, *22*(1), 789–817. https://doi.org/10.5194/hess-22-789-2018

Jaramillo, F., & Destouni, G. (2015). Local flow regulation and irrigation raise global human water consumption and footprint. *Science*, *350*(6265), 1248–1251. https://doi.org/10.1126/science.aad1010

Johnson, S. A., Stedinger, J. R., & Staschus, K. (1991). Heuristic operating policies for reservoir system simulation. *Water Resources Research*, *27*(5), 673–685. https://doi.org/10.1029/91wr00320

Lamarche, C., Santoro, M., Bontemps, S., d'Andrimont, R., Radoux, J., Giustarini, L., et al. (2017). Compilation and validation of SAR and optical data products for a complete and global map of inland/ocean water tailored to the climate modeling community. *Remote Sensing*, *9*(1), 36. https://doi.org/10.3390/rs9010036

Lehner, B., & Döll, P. (2004). Development and validation of a global database of lakes, reservoirs and wetlands. *Journal of Hydrology*, *296*(1), 1–22. https://doi.org/10.1016/j.jhydrol.2004.03.028

Lehner, B., Liermann, C. R., Revenga, C., Vörösmarty, C., Fekete, B., Crouzet, P., et al. (2011). High-resolution mapping of the world's reservoirs and dams for sustainable river-flow management. *Frontiers in Ecology and the Environment*, *9*(9), 494–502. https://doi.org/10.1890/100125

Lehner, B., Verdin, K., & Jarvis, A. (2008). New global hydrography derived from spaceborne elevation data. *Eos Transactions American Geophysical Union*, *89*(10), 93–94. https://doi.org/10.1029/2008eo100001

Leng, G., Leung, L. R., & Huang, M. (2017). Significant impacts of irrigation water sources and methods on modeling irrigation effects in the ACME L and Model. *Journal of Advances in Modeling Earth Systems*, *9*(3), 1665–1683. https://doi.org/10.1002/2016MS000885

Lobell, D., Bala, G., Mirin, A., Phillips, T., Maxwell, R., & Rotman, D. (2009). Regional differences in the influence of irrigation on climate. *Journal of Climate*, *22*(8), 2248–2255. https://doi.org/10.1175/2008JCLI2703.1

Milly, P. C. D., Betancourt, J., Falkenmark, M., Hirsch, R. M., Kundzewicz, Z. W., Lettenmaier, D. P., & Stouffer, R. J. (2008). Stationarity is dead: Whither water management? *Science*, *319*(5863), 573–574. https://doi.org/10.1126/science.1151915

Müller Schmied, H., Cáceres, D., Eisner, S., Flörke, M., Herbert, C., Niemann, C., et al. (2021). The global water resources and use model WaterGAP v2.2d: Model description and evaluation. *Geoscientific Model Development, 14*, 1037–1079. https://doi.org/10.5194/gmd-14-1037-2021

MWR. (2001). China water resources Bulletins of 2000 (in Chinese) (Tech. Rep.). Ministry of Water Resources.

MWR. (2020). China water resources Bulletins of 2019 (in Chinese) (Tech. Rep.). Ministry of Water Resources.

Nalbantis, I., & Koutsoyiannis, D. (1997). A parametric rule for planning and management of multiple-reservoir systems. *Water Resources Research*, *33*(9), 2165–2177. https://doi.org/10.1029/97wr01034

Neverre, N., Dumas, P., & Nassopoulos, H. (2016). Large-scale water scarcity assessment under global changes: Insights from a hydroeconomic framework. *Hydrology and Earth System Sciences Discussions*, 1–26. https://doi.org/10.5194/hess-2015-502

Ngo-Duc, T., Laval, K., Ramillien, G., Polcher, J., & Cazenave, A. (2007). Validation of the land water storage simulated by organizing carbon and hydrology in dynamic ecosystems (ORCHIDEE) with gravity recovery and climate experiment (GRACE) data. *Water Resources Research*, *43*(4), 1–8. https://doi.org/10.1029/2006WR004941

Nguyen-Quang, T., Polcher, J., Ducharne, A., Arsouze, T., Zhou, X., Schneider, A., & Fita, L. (2018). ORCHIDEE-ROUTING: Revising the river routing scheme using a high-resolution hydrological database. *Geoscientific Model Development*, *11*(12), 4965–4985. https://doi.org/10.5194/gmd-11-4965-2018

NPC. (2011). Outline of the 12th five-year plan for the national economic and social development of the people's Republic of China (title only, in Chinese) (Tech. Rep.). National People's Congress. Retrieved from http://www.gov.cn/2011lh/content_1825838.htm

Poff, N. L., Richter, B. D., Arthington, A. H., Bunn, S. E., Naiman, R. J., Kendy, E., et al. (2010). The ecological limits of hydrologic alteration (ELOHA): A new framework for developing regional environmental flow standards. *Freshwater Biology*, *55*(1), 147–170. https://doi.org/10.1111/j.1365-2427.2009.02204.x

Poff, N. L., & Zimmerman, J. K. H. (2010). Ecological responses to altered flow regimes: A literature review to inform the science and management of environmental flows. *Freshwater Biology*, *55*(1), 194–205. https://doi.org/10.1111/j.1365-2427.2009.02272.x

Pokhrel, Y. N., Hanasaki, N., Wada, Y., & Kim, H. (2016). Recent progresses in Incorporating human land-water management into global land surface models toward their integration into Earth system models: Recent Progresses in incorporating human land-water management into global land surface models. *Wiley Interdisciplinary Reviews: Water*, *3*(4), 548–574. https://doi.org/10.1002/wat2.1150

Rost, S., Gerten, D., Bondeau, A., Lucht, W., Rohwer, J., & Schaphoff, S. (2008). Agricultural green and blue water consumption and its influence on the global water system. *Water Resources Research*, *44*(9). https://doi.org/10.1029/2007WR006331

Scherer, L., & Pfister, S. (2016). Global water footprint assessment of hydropower. *Renewable Energy*, *99*, 711–720. https://doi.org/10.1016/j.renene.2016.07.021

Schrapffer, A., Sörensson, A., Polcher, J., & Fita, L. (2020). Benefits of representing floodplains in a land murface Model: Pantanal simulated with ORCHIDEE CMIP6 version. *Climate Dynamics*, *55*(5–6), 1303–1323. https://doi.org/10.1007/s00382-020-05324-0

Shaffer, K. H., & Runkle, D. L. (2007). Consumptive water-use coefficients for the Great Lakes basin and climatically similar areas (Tech. Rep. No. 2007-5197). USGS. Retrieved from https://pubs.usgs.gov/sir/2007/5197/pdf/SIR2007-5197_low-res_all.pdf

Siebert, S., Henrich, V., Frenken, K., & Burke, J. (2013). *Update of the digital global map of irrigation areas to version 5*. Institute of Crop Science and Resource Conservation, University of Bonn, Germany; Land and Water Division, Food and Agriculture Organization of the United Nations. https://doi.org/10.13140/2.1.2660.6728

Sutanudjaja, E. H., van Beek, R., Wanders, N., Wada, Y., Bosmans, J. H. C., Drost, N., et al. (2018). PCR-GLOBWB 2: A 5 arcmin global hydrological and water resources model. *Geoscientific Model Development*, *11*(6), 2429–2453. https://doi.org/10.5194/gmd-11-2429-2018

van Beek, L. P. H., Wada, Y., & Bierkens, M. F. P. (2011). Global monthly water stress: 1. Water balance and water availability: Global Monthly Water Stress, 1. *Water Resources Research*, *47*(7). https://doi.org/10.1029/2010wr009791

Verdin, K. L., & Verdin, J. P. (1999). A topological system for delineation and codification of the Earth's river basins. *Journal of Hydrology*, *218*(1–2), 1–12. https://doi.org/10.1016/S0022-1694(99)00011-6

Vicente-Serrano, S. M., Peña-Gallardo, M., Hannaford, J., Murphy, C., Lorenzo-Lacruz, J., Dominguez-Castro, F., et al. (2019). Climate, irrigation, and land cover change explain streamflow trends in countries bordering the northeast Atlantic. *Geophysical Research Letters*, *46*(19), 10821–10833. https://doi.org/10.1029/2019GL084084

Voisin, N., Li, H., Ward, D., Huang, M., Wigmosta, M., & Leung, L. R. (2013). On an improved sub-regional water resources management representation for integration into earth system models. *Hydrology and Earth System Sciences*, *17*(9), 3605–3622. https://doi.org/10.5194/hess-17-3605-2013

Wada, Y., Bierkens, M. F. P., de Roo, A., Dirmeyer, P. A., Famiglietti, J. S., Hanasaki, N., et al., (2017). Human-water interface in hydrological modelling: Current status and future directions. *Hydrology and Earth System Sciences*, *21*(8), 4169–4193. https://doi.org/10.5194/hess-21-4169-2017

Wada, Y., van Beek, L. P. H., & Bierkens, M. F. P. (2012). Nonsustainable groundwater sustaining irrigation: A global assessment. *Water Resources Research*, *48*(6). https://doi.org/10.1029/2011wr010562

Wang, F., Ge, Q., Yu, Q., Wang, H., & Xu, X. (2017). Impacts of land-use and land-cover changes on river runoff in Yellow River basin for period of 1956-2012. *Chinese Geographical Science*, *27*(1), 13–24. https://doi.org/10.1007/s11769-017-0843-3

Wang, X.-J., Zhang, J.-Y., Shahid, S., Yu, L., Xie, C., Wang, B.-X., & Zhang, X. (2018). Domestic water demand forecasting in the Yellow river basin under changing environment. *International Journal of Climate Change Strategies and Management*, *10*(3), 379–388. https://doi.org/10.1108/IJCCSM-03-2017-0067

Yin, Z., Wang, X. H., Ottlé, C., Zhou, F., Guimberteau, M., Polcher, J., et al. (2020). Improvement of the irrigation scheme in the Orchidee land surface model and impacts of irrigation on regional water budgets over china. *Journal of Advances in Modeling Earth Systems*, *12*(4), e2019MS001770. https://doi.org/10.1029/2019MS001770

Yoshikawa, S., Cho, J., Yamada, H. G., Hanasaki, N., & Kanae, S. (2014). An assessment of global net irrigation water requirements from various water supply sources to sustain irrigation: Rivers and reservoirs (1960–2050). *Hydrology and Earth System Sciences*, *18*(10), 4289–4310. https://doi.org/10.5194/hess-18-4289-2014

Zhou, F., Bo, Y., Ciais, P., Dumas, P., Tang, Q., Wang, X., et al. (2020). Deceleration of China's human water use and its key drivers. *Proceedings of the National Academy of Sciences of the United States of America*, *117*, 7702. https://doi.org/10.1073/pnas.1909902117

Zhou, X., Polcher, J., Yang, T., Hirabayashi, Y., & Nguyen-Quang, T. (2018). Understanding the water cycle over the upper Tarim basin: Retrospecting the estimated discharge bias to atmospheric variables and model structure. *Hydrology and Earth System Sciences*, *22*(11), 6087–6108. https://doi.org/10.5194/hess-22-6087-2018